SYNTHESIS AND APPLICATION OF CALCIUM OXIDE (CaO) NANOPARTICLES FROM SNAIL SHELLS (*ARCHACHATINA MARGINATA*) IN INDUSTRIAL PAINT EFFLUENT

BY

TRACY OKODUWA

PSC1908673

DEPARTMENT OF CHEMISTRY,

FACULTY OF PHYSICAL SCIENCE,

UNIVERSITY OF BENIN,

BENIN-CITY.

APRIL, 2024

A RESEARCH PROJECT ON THE

SYNTHESIS AND APPLICATION OF CALCIUM OXIDE (CaO) NANOPARTICLES FROM SNAIL SHELLS (*ARCHACHATINA MARGINATA*) IN INDUSTRIAL PAINT EFFLUENT

BY

TRACY OKODUWA

PSC1908673

A PROJECT SUBMITTED TO THE DEPARTMENT OF CHEMISTRY, FACULTY OF PHYSICAL SCIENCE, UNIVERSITY OF BENIN, BENIN CITY, EDO STATE IN PARTIAL FULFILLMENT OF THE REQUIREMENTS FOR THE AWARD OF BACHELOR OF SCIENCE (B.SC)

APRIL, 2024

CERTIFICATION

This is to certify that this project work was carried out by **TRACY OKODUWA** in the Department of Chemistry, Faculty of Physical Science, University of Benin, Benin City, in partial fulfilment for the award of Bachelor of Science (B.Sc.) degree in Chemistry.

Tracy Okoduwa (Student)	Date
Prof. Mrs. E.U. Ikhuoria (Project Supervisor)	Date
Prof. J.U. Iyasele (Head of Department)	Date

DEDICATION

This work is dedicated, first and foremost, to God, the sustainer of life, whose presence has guided me and bestowed upon me wisdom and favor throughout my journey in this program. I am also deeply grateful to my family, and in particular, my lovely mother, MRS. ANITA AGHEDO for her unwavering care, love, and support have been a constant source of strength and encouragement. Also to my aunt MRS. BOSE LUGBENWEI for her support throughout this program. This work is a reflection of their enduring influence and support in my life.

ACKNOWLEDGEMENT

I would like to express my sincere gratitude to the Almighty God for His grace, wisdom, and strength that sustained me throughout the course of this research.

I am deeply grateful to my project supervisor, Prof. Mrs. E.U. Ikhuoria, for her invaluable guidance, support, and encouragement. Her expertise and insights have been instrumental in shaping this work and expanding my understanding of my research work.

I would also like to extend my appreciation to the Head of Department, Prof. J.U. Iyasele, for his support and encouragement throughout my academic journey. His mentorship and guidance have been invaluable.

Special thanks to my best friend, Perfect Osahon Isibor, for his unwavering support, encouragement, and invaluable assistance throughout this project. His insightful feedback, encouragement, and dedication have been a constant source of motivation.

Am also thankful to my group members and friends for their support and encouragement throughout this project.

Finally, I would like to thank my family for their love, support, and understanding during this challenging yet rewarding journey.

ABSTRACT

This research study explores the innovative use of waste materials (snail shells) for the treatment of industrial paint effluent. Paint effluent, known for its complex composition of heavy metals, organic solvents, and suspended solids, poses significant environmental challenges. Nanomaterials due to their unique properties, high reactivity and high surface area to volume ratio, offers promising solutions for efficient wastewater treatment. The synthesis, optimization, and application of calcium oxide (CaO) nanoparticles derived from waste snail shells was investigated. The nanoparticles were synthesized via the sol-gel method and characterized using Fourier transform infrared spectroscopy (FTIR), dynamic light scattering (DLS), X-ray diffraction (XRD), and scanning electron microscopy (SEM). Response surface methodology (RSM) with central composite design (CCD), was used to optimize the treatment conditions (pH, contact time, and adsorbent dosage), with the optimum values determined as pH 7, contact time of 52.5 minutes, and CaO-NPs dosage of 5.5 g/L. This optimized condition achieved a remarkable 98.1091% contaminants removal efficiency. This study not only demonstrates the efficacy of CaO nanoparticles for paint wastewater treatment but also underscores the sustainable approach of utilizing waste materials to treat waste. The cost efficiency of this method further highlights its potential for practical application in environmental remediation efforts.

TABLE OF CONTENTS

LIST OF FIGURES

LIST OF TABLES

CHAPTER ONE

INTRODUCTION AND LITERATURE REVIEW

1.1 INTRODUCTION

Nanotechnology is a discipline which focuses on innovations that operate at the nanoscale and have numerous practical uses. It works with at least one-dimensional nanomaterials with sizes ranging from 1 to 100 nm (*Khan et al.,, 2019*). Since the 1980s, extensive research in the field of nanotechnology has continued to be a modern marvel of scientific discovery. Studies on nanotechnology are widely applied in our daily lives and are ushering in a new age for the society as a whole (*Nizamuddin et al., 2018*). The application of nanotechnology in water and wastewater remediation has grown beyond its expectations. Studies have shown that nanotechnology is a viable and cost-effective substitute for traditional methods in the removal of pollutants like inorganics (heavy metals), organic and microorganisms from water and wastewater. They are useful for the purification of water and wastewater because of their capacity to oxidize, precipitate, reduce, and adsorb pollutants like heavy metals, nitroaromatic compounds, inorganic anions, phosphates, radio elements, nitrates, phenols, organic dyes, and chlorinated and halogenated organic compounds (*Araujo et al., 2015)*.

Industrial activities generates diverse array of effluents, and paint water effluent stands out as one of the main contributors to environmental pollution. Their diverse compositions, which includes organic and inorganic contaminants can have long term implications on the ecosystem and human health, and disposal of such effluents can be difficult (*Mostafaie et al., 2021)*. Safely treating this wastewater before being disposed to natural water sources is essential for attaining the UN SDGs, particularly Goal 14: Life under water. Innovative and long-lasting solutions must be developed as

conventional treatment methods may not be sufficient to address the variety of pollutants found in paint water effluent. In order to address this problem, this study investigates the use of calcium oxide (CaO) nanoparticles, synthesized via the Sol-gel method utilizing snail shells as a sustainable precursor for calcium ions. The use of snail shells is in line with green chemistry principles, which encourages the recycling of waste materials.

1.1.1 BACKGROUND OF STUDY

The most significant and limited resource on Earth is water, which has been continuously polluted due to the rapid industrialization and population increase in the last decades, through the release of heavy metals, and numerous organic and inorganic pollutants (*Chaturvedi et al., 2020*). The major sources of water contamination are sewage water, industrial effluent, incorrect application of pesticides and fertilizers, and oil spills in agricultural system. Amongst these, industrial effluent stands out as a significant source of pollution with major economical impact due to the presence of chemicals and heavy metals. Industrial effluents such as paint effluent contains heavy metals which are non-biodegradable causing them to accumulate in living things both animals and plants, posing a serious threat to human health (*Afroze and Sen, 2018*).

Numerous treatment techniques have been adopted to remove heavy metals and other pollutants from wastewater. Chemical precipitation, membrane filtration (including reverse osmosis and electrodialysis), electrolytic procedures, coagulation or flocculation, ion exchange, adsorption, and biological sorption are a few of the various techniques for removing pollutants, however, these methods are costly and have major drawbacks which includes; huge amount of chemical reagents and high energy requirements, creation of toxic sludge or other wastewater products (secondary pollution), and poor treatment effectiveness at low metal ion concentration, particularly when the concentration of heavy metals in wastewater is low (<100 ppm). Adsorption is the most preferred

technique due to its simplicity, flexible design and easy operation (*El-sayed et al., 2020*). Due to its superior sorption capacity, activated carbon is one of the most researched and effective adsorbents available. However, due to cost, poor selectivity, and difficulties of regeneration, its application is limited causing researchers to focus on metal and metal-oxide based nanomaterials (*Deliyanni et al., 2015*).

The utilization of nanoparticles in the treatment of water and wastewater has attracted a lot of attention. Nanomaterials are highly reactive and have great adsorption capacities due to their small sizes and consequently large specific surface areas. Furthermore, nanoparticles have a high degree of mobility in solutions (*Khin et al., 2012*). Organic pollutants, heavy metals, inorganic anions, and microorganisms have been to be successfully removed using nanomaterials. Without requiring the deployment of extra systems, utilization of nanomaterials have demonstrated a high degree superiority over traditional methods in the area of wastewater treatment (*Konyukhov, 2018*). Additionally, nanomaterials are devoid of features associated with secondary pollution making it a preferable technique.

Several techniques have been used to synthesize these metal oxide nanoparticles, such as the ultrasonic-assisted method, the hydrogen plasma-metal reaction method, the biopolymer-assisted method, microwave-assisted method, facial calcination, co-precipitation, direct thermal decomposition, chemical co-precipitation, two-step process(green synthesis) and two step thermal decomposition. Most of these techniques have drawbacks, which includes the need for additives, high pressure and temperature, as well as time-consuming, costly, and difficult procedures. Most of the shortcomings of the aforementioned techniques are addressed by the sol-gel method. It doesn't require expensive equipment and is easy, and time-efficient. It can also be done without pressure and at a lower temperature. The sol-gel method is more widely used and has more

industrial applications than other currently available methods (*Feinle et al., 2016*). Therefore, it is a promising method for the synthesis of calcium oxide nanoparticles. Snail shells are employed as a sustainable and cost-effective source of calcium ions for the synthesis of calcium oxide nanoparticles using the sol gel method, which can have various applications, including in the treatment of wastewater. This approach is inexpensive, simple, and eco-friendly.

1.1.2 STATEMENT OF PROBLEM

Industrial effluent, particularly from paint manufacturing processes, poses significant environmental and health impact due to its complex composition and diverse contaminants, including heavy metals, organic solvents, and suspended solids (*Chen et al., 2020*).

Despite the availability of various treatment methods, including chemical precipitation, coagulation-flocculation, and membrane filtration, these conventional approaches often exhibit shortcomings that hinder their effectiveness in treating paint wastewater. Some of these shortcomings includes; inadequate removal efficiency, limited selectivity, high operational costs, environmental impact, limited sustainability, etc.

In light of these shortcomings, this research intends to investigate ways by which waste materials such as snail shells can be utilized for the production of CaO nanoparticles for contaminant removal in paint effluent, addressing the limitations of conventional treatment methods.

1.1.3 RELEVANCE OF THE RESEARCH

This research is relevant as it focuses on the synthesis, optimization, and application of CaO nanoparticles from snail shells for the treatment of industrial paint effluent. By optimizing the synthesis and treatment conditions, this research aims to develop a cost-effective and efficient method for treating paint effluent, which can be applicable to other industries facing similar wastewater treatment challenges (*Kim & Kang, 2020*). This research offers several advantages over traditional approaches, as highlighted below:

- **Enhanced Treatment Efficiency:** CaO nanoparticles exhibit high surface area and reactivity, allowing for efficient adsorption and degradation of organic pollutants and heavy metals present in paint wastewater compared to conventional methods (*Zhang et al., 2019*).
- **Cost-effectiveness and Sustainability:** The synthesis of CaO nanoparticles from snail shells provides a cost-effective and environmentally sustainable alternative to conventional treatment methods (*Li et al., 2017*). Snail shells are abundant and renewable resources, and their utilization minimizes the reliance on expensive chemical reagents and energy-intensive processes.
- **Minimization of Secondary Waste:** CaO nanoparticles offer the advantage of generating minimal secondary waste compared to conventional treatment methods (*Yang et al., 2020*).

1.1.4 SCOPE OF WORK

This research will encompass the following key aspects:

- Implement the sol-gel method for the synthesis of calcium oxide nanoparticles from snail shells, ensuring precise control over reaction parameters to achieve reproducibility.

- Analyzing the synthesized Calcium oxide nanoparticles using characterization techniques such as XRD, FTIR, SEM and DLS.
- Investigate variables such as contact time, pH, and adsorbent dosage to identify optimal conditions using Response Surface Methodology (RSM).
- Evaluate the efficiency of the synthesized nanoparticles in treating paint wastewater, with a specific emphasis on contaminant removal.

1.1.5 AIM AND OBJECTIVES

The aim of this research is to develop a sustainable, environmental friendly and effective technique for the treatment of industrial paint effluent through the synthesis of calcium oxide nanoparticles from snail shells.

To achieve the above aim, the study is guided by the following specific objectives. To:

1. synthesize calcium oxide nanoparticles from snail shells, ensuring a controlled and reproducible process employing the Sol-gel method.
2. characterize the synthesized nanoparticles, utilizing advanced techniques such as X-Ray Diffraction (XRD) analysis, Dynamic light scattering (DLS), Scanning Electron Microscopy (SEM) and FTIR spectroscopy to gain a deeper understanding of the material composition.
3. optimize the treatment conditions for the removal of contaminants from industrial paint wastewater using Response Surface Methodology (RSM) with Central Composite Design (CCD), considering factors such as pH, contact time, and adsorbent dosage.

1.2 LITERATURE REVIEW

1.2.1 Review of related work

The treatment of industrial effluent has been a topic of extensive research due to its environmental and health implications. Nanotechnology, particularly the use of nanomaterials, has emerged as a promising approach for the removal of various contaminants from wastewater. Several studies have explored the use of different types of nanomaterials and their applications in wastewater treatment.

One of the commonly studied nanomaterials is titanium dioxide (TiO2) nanoparticles. TiO2 nanoparticles have been shown to be effective in the removal of organic pollutants from wastewater through photocatalytic degradation. For example, (*Singh et al., 2016*) investigated the photocatalytic degradation of organic dyes using TiO2 nanoparticles and reported high degradation efficiencies, highlighting the potential of TiO2 nanoparticles in wastewater treatment.

In addition to TiO2 nanoparticles, iron-based nanoparticles have also been extensively studied for wastewater treatment. Iron nanoparticles have been shown to effectively remove heavy metals from wastewater through adsorption and co-precipitation processes. (*Thilakan et al., 2022*) demonstrated the removal of lead and cadmium from wastewater using iron nanoparticles. synthesized from waste materials, indicating the potential for sustainable wastewater treatment practices.

Moreover, the use of natural materials for the synthesis of nanoparticles has gained attention due to their low cost and environmental benefits. Egg shells, for example, have been utilized for the synthesis of calcium oxide (CaO) nanoparticles. CaO nanoparticles derived from egg shells have shown promising adsorption capacities for various heavy metals in wastewater (*Kasirajan et al., 2022*).

Overall, these studies emphasize the potential of nanomaterials for wastewater treatment and highlight the importance of further research in this area. By building upon these existing studies, this research aims to contribute to the development of sustainable and efficient approach to treatment of industrial effluent using nanotechnology.

1.2.2 Nanoscience and Nanotechnology

Nanoscience is a branch of science that comprises of the study of the properties of matter at the nanoscale (*Mulvaney, 2015*).

Nanotechnology is the branch that comprises the synthesis, engineering, and utilization of materials whose size ranges from 1 to 100 nm, known as nanomaterials (*Hasan, 2015*).

The birth of nanoscience and nanotechnology concepts is usually traced back to the famous lecture of Nobel laureate Richard Feynman at the 1959 meeting of the American Physical Society, ‘‘There’s Plenty of Room at the Bottom’’ (*Feynman, 1959*) However, the application of nanotechnology and nanomaterials goes back in history long before that.

1.2.3 Reasons why nanomaterials are Unique

Nanomaterials are employed in many different fields today, including agriculture, energy storage, water treatment, catalysis, and medicine, among others, because of their unique properties (*Bratovcic, 2019*). The two key factors that causes the remarkable difference in the behavior of

nanomaterials from the same materials at larger dimensions are; surface effects and quantum effects (*Roduner, 2006*). These factors cause nanomaterials to display novel mechanical, thermal, magnetic, catalytic, electrical, and optical properties as well as increased catalytic activity (*Gade et al., 2010*) compared to their bulk materials.

The physical and chemical properties of nanomaterials differ from those of their larger-dimension counterparts as a result of each of these differences. The reactivity of nanomaterials generally increases due to their larger surface areas and larger surface-to-volume ratios which results in larger reaction surface (*Buzea et al., 2007*).

Unique size-dependent properties of nanomaterials are observed in the 1–100 nm region where quantum phenomena are present. That is, by shrinking the size of the material, quantum effects become more apparent and nanomaterials become quanta. Certain non-magnetic bulk materials, like palladium, platinum, and gold, become magnetic at the nanoscale due to quantum confinement effects, (*Roduner, 2006*).

1.2.4 Classification of nanomaterials

Materials that have at least one dimension in the nanoscale (that is, smaller than 100 nm) are referred to as nanomaterials (*Kolahalam et al., 2019*). Nanomaterials are classified into four groups based on their dimensionalities as discussed below:

- Zero-dimensional nanomaterials (0-D): the nanomaterials in this class have all their three dimensions in the nanoscale range. Examples are quantum dots, fullerenes, and nanoparticles.

- One-dimensional nanomaterials (1-D): the nanomaterials in this class have one dimension outside the nanoscale. Examples are nanotubes, nanofibers, nanorods, nanowires, and nanohorns.
- Two-dimensional nanomaterials (2-D): the nanomaterials in this class have two dimensions outside the nanoscale. Examples are nanosheets, nanofilms, and nanolayers.
- Three-dimensional nanomaterials (3-D) or bulk nanomaterials: in this class the materials are not confined to the nanoscale in any dimension. This class contains bulk powders, dispersions of nanoparticles, arrays of nanowires and nanotubes, etc.

1.2.5 Nanoparticles (NPs)

Nanoparticles are defined by the International Organization for Standardization (ISO) as nano-objects having all external dimensions in the nanoscale. Terms like nanofibers or nanoplates may be preferred over NPs if the dimensions differ significantly (usually by more than three times). NPs can be of different sizes, shapes, and structures. NPs can range in size from 1-100 nm. When NPs are smaller than 1 nm, the phrase "atom clusters" is typically used. NPs can be amorphous or crystalline, containing single or many crystal solids. NPs may be loose or agglomerated (*Machado et al., 2015*).

1.2.6 Classification of nanoparticles

NPs are generally grouped into three classes, based on their composition: organic, carbon-based, and inorganic (*Ealia and Saravanakumar, 2017*).

- **Organic NPs**

NPs composed of proteins, carbohydrates, lipids, polymers, or any other organic component fall into this class (*Pan and Zhong, 2016*). Dendrimers, liposomes, micelles, and protein complexes like ferritin are the most well-known examples of this class. Most of these NPs are biodegradable and non-toxic.

- **Carbon-based NPs**

NPs consisting entirely of carbon atoms fall under this class. Carbon black nanoparticles, carbon quantum dots, and fullerenes are common examples of this class. Carbon-based nanoparticles (NPs) have a wide range of applications, including drug delivery, energy storage, bioimaging, photovoltaic devices, and environmental sensing applications to monitor microbial ecology or detect microbial pathogens (*Mauter and Elimelech, 2008*). These applications are made possible by their unique electrical conductivity, high strength, electron affinity, optical, thermal, and sorption properties. More sophisticated carbon-based NPs are nanodiamonds and carbon nanoonions.

- **Inorganic NPs**

NPs that are not composed of carbon or organic materials fall under this class. Common examples includes semiconductor, ceramic, and metal nanoparticles. Metal NPs can be monometallic, bimetallic, or polymetallic, and they are entirely composed of metal precursors. These NPs have distinct optical and electrical properties because of their localized surface plasmon resonance features (*Khan et al., 2019*).

1.2.7 Physicochemical properties of NPs

As previously stated, NPs' distinct physical and chemical features, which are absent from their larger-dimension counterparts of the same materials, make them suitable for a wide range of applications. This sections provide an overview of the key physicochemical properties that changes on the nanoscale.

1.2.7.1 Mechanical properties

The mechanical properties of nanomaterials typically include the following ten elements: strength, brittleness, hardness, toughness, fatigue strength, plasticity, elasticity, ductility, rigidity, and yield stress (*Wu et al., 2020*). NPs exhibit distinct mechanical properties due to surface and quantum effects. For instance, ultrafine FeAl alloy powder exhibits improved plasticity, strength and ductility whereas conventional FeAl powder which is composed of microparticles (larger than 4 μm), is brittle (*Pithawalla et al., 2001*). It is believed that these unique features arises due to the diverse interaction forces between NPs or between them and a surface.

1.2.7.2 Magnetic properties

Many materials becomes magnetic in the nanoscale due to uneven electronic distribution. For example, FeAl is not magnetic in bulk but becomes magnetic in the form of nanoparticles (*Pithawalla et al., 2001*), other examples are Au and Pd. However, at the nanoscale, two other key factors; size and shape heavily influences the magnetic properties.

1.2.7.3 Electronic and optical properties

The size, shape, and dielectric environment of NPs are generally related to their optical characteristics. Based on the size of Ag NPs, experimental investigations revealed notable differences in their optical properties. The primary extinction peak for Ag NPs with a 30 nm radius was found at a wavelength of 369 nm, but a completely different behavior was noted for Ag NPs with a 60 nm radius (*Kelly et al., 2003*). The same researchers also observed that NP shape is important for the optical properties.

1.2.7.4 Thermal properties

The size of NPs directly affects their electrical and thermal conductivity (*Andrievski, 2014*). As NP size decreases, the ratio of surface area to volume increases hyperbolically. This larger surface-to-volume ratio provides more electrons for heat transfer compared to bulk materials, as electron conduction is a key heat transport mechanism (*Qiu et al., 2020*).

1.2.7.5 Catalytic properties

NP catalysts often exhibit novel or significantly enhanced catalytic properties, such as selectivity and reactivity, compared to their bulk materials. The catalytic properties of NPs are influenced by factors such as size, shape, composition, interparticle spacing, and oxidation state. (*Haruta, 2004; Henry, 2005*)

1.2.8 Nanoparticles Synthesis

Traditionally, there are two methods for creating nanoparticles which can be classified based on their assembly i.e., Top-down and Bottom-up approach.

1.2.8.1 Top-down approach

The methods begin with bulk block materials which are reduced to nanoparticles after a sequence of operations performed over them. Top-down approaches are typically simpler, relying on bulk material elimination or bulk fabrication technique miniaturization to create the desired structure with the desired properties. Main shortcomings of these methods are that they involve large installations and huge capital is required for set up and is therefore not suitable for large-scale production but is suitable for laboratory experimentation. The methods in top-down approach includes mainly the physical methods of nanoparticle synthesis.

1.2.8.2 Bottom-up Approach

The bottom-up approach involves constructing a material from the smallest units, such as atoms, molecules, or clusters, and is frequently employed in the production of nanoscale materials. The process allows for the creation of uniform shapes, sizes, and distributions in many nanoscale materials. The methodology is principally based on the principle of molecular recognition (self-assembly). Bottom-up nanofabrication has the potential to be considerably more cost-effective than top-down nanofabrication (*Abid et al., 2021*).

1.2.9 Methods of synthesis of nanoparticles

Various chemical, physical and biological techniques are utilized to synthesize various varieties of nanoparticles. Depending upon the application, the methods for synthesis of nanoparticles are selected. Every method has some advantages as well as disadvantages; the production method is selected based upon the availability of the facilities.

1.2.9.1 Chemical Method

The chemical method is characterized by low cost, simple operation, and strong scalability. These methods are classified as bottom-up nanoparticle synthesis. They include microwave assisted synthesis, Hydrothermal synthesis, polyol synthesis, micro emulsion technique, salvo thermal synthesis, plasma and chemical vapors synthesis, etc. Among these methods, the Sol-gel technique stands out as a versatile approach for producing nanoparticles with precise control over their size, shape, and composition.

1.2.9.1.1 Sol-Gel Method

This method comprises of the condensation and hydrolysis of metal alkoxides or suitable metal precursors in solution. A stable solution is formed, known as the sol. Upon hydrolysis or condensation, the gel is formed with increased viscosity, followed by drying or calcination to obtain nanoparticles. Compared to other methods of nanoparticles synthesis, the Sol-gel process allows for precise control over the size, shape, and composition of nanoparticles by adjusting synthesis parameters such as precursor concentration, pH, temperature, solvent composition, reaction conditions. This level of control enables the production of nanoparticles with tailored properties to meet specific application requirements. This technique is extensively useful for the synthesis of metal oxide nanoparticles for diverse industrial and biomedical applications.

1.2.9.1.2 Co-precipitation method

It is a wet chemical process, also called a solvent displacement method. Polymer phase can be synthetic or natural; polymer solvents are ethanol, acetone, hexane, and non-solvent polymer. Nanoparticles are produced by rapid diffusion of polymer-solvent into a non-solvent polymer

phase by mixing the polymer solution at last. Nanoparticles are produced by interfacial tension at two phases (*Das and Srivasatava, 2016*).

1.2.9.1.3 Hydrothermal synthesis

Hydrothermal synthesis involves a broad temperature range from room temperature to very high temperatures for the synthesis of nanoparticles. It is a promising method for producing hydrophobic or hydrophilic magnetic nanoparticles with controlled size and shape. This method of synthesis can yield monodisperse particles with high crystallinity; however, it may be difficult to scale in some cases. The benefit of using this technique is that it enables the low-cost synthesis of large number of NPs (*Banerjee et al., 2008*).

1.2.9.1.4 Solvothermal synthesis

It has been found that solvothermal synthesis is a versatile technique for creating a wide variety of nanoparticles with a narrow size distribution. Similar to the hydrothermal approach, the solvothermal method is applicable to solvents other than water. The solvothermal technique has been utilized to produce nanoparticles and nanorods with and without surfactants, offering greater control over form, size, and crystallinity distributions compared to the hydrothermal process. (*Byun et al., 2011*).

1.2.9.1.5 Polyol Synthesis

The polyol process is a metal-containing compound synthesis technique that uses a reaction medium, polyethylene glycol acts as a solvent, complexing agent and reducing agent. A polyol

solution dissolves the metal precursor, heated to almost freezing points (temperature). Also, at the high temperatures used in the reactions described here, the polyol serves as a reducing agent for the reduction of metal (*Meshesha et al., 2009*).

1.2.9.1.6 Chemical vapor deposition

The chemical vapor deposition method (CVD) involves a chemical reaction. CVD procedure is mostly used in semiconductor manufacturing for depositing thin films of different materials. This method involves one or more volatile precursors, the substrate is exposed to those precursors that decompose on it and form the desired deposit. The CVD method can synthesize ultrafine particles of less than 1 μm by the chemical reaction taking place in the gaseous phase. The reaction can be controlled to produce nanoparticles of size ranging from 10 to 100 nm.

1.2.9.2 Physical Method

Nanoparticles have traditionally been produced using physical methods, which utilize thermal energy, high-energy radiation and mechanical pressure, to cause material condensation, evaporation, abrasion, or melting. Physical methods employs top-down approach, are solvent-free, and yield consistent monodisperse nanoparticles. Laser ablation, laser pyrolysis, physical vapor deposition, high-energy ball milling, and spluttering are among the physical methods commonly used to generate nanoparticles.

1.2.9.2.1 Laser ablation

In the laser ablation process, particles from the material are evaporated using a powerful laser beam. (*Kim et al., 2017*). The setup is an ultra high vacuum equipped with inert or reactive gas introduction facility, laser beam, solid target and cooled substrate. The target sample is placed inside a vacuum chamber. The high-pulsed laser beam is focused on the sample and plasma is generated, which is formerly transformed into a colloidal solution of nanoparticles. The second-harmonic group type laser is frequently used to formulate nanoparticles.

1.2.9.2.2 Mechanical (Ball Milling)

It is a top-down approach for preparation of nanoparticles by applying mechanical energy. This involves crushing of solid materials using hardened steel, silicon carbide (SiC) or tungsten carbide (WC) balls in stainless steel container. The crushing is carried out for 100 to 150 hours to get uniform powder. This method is simple, cheap and produces nanoparticles of 2-20 nm range however, problems like control on shape and purity exists. (*Kumar and Pattammattel, 2017*).

1.2.9.2.3 Pulsed wired discharge method

This is the most widely used physical method for synthesis of metal nanoparticles. A metal wire is vaporized by a pulsated current to yield a vapour, which is then cool by ambient gas to procedure nanoparticles. This scheme has possibly a high fabrication speed and high energy productivity.

1.2.9.2.4 Laser pyrolysis

The process of synthesis of nanoparticles by using a laser is known as laser pyrolysis. Laser pyrolysis is an effective method for synthesizing inexpensive and magnetic nanoparticles (*Amato et al., 2013*). An intense laser beam is focused to decompose the mixture of reactant gases in the

presence of some inactive gas like helium or argon. The gas pressure shows a significant part in determining the particle sizes and their distribution.

1.2.9.2.5 Spluttering

This is a top-down process of nanoparticles synthesis in which a solid surface is bombarded with high energy particles (Argon ions) resulting in surface erosion of the solid surface with formation of atoms due to collision of energetic particles and the solid surface.

1.2.9.2.6 Thermal evaporation condensation

It is top-down method which is used for synthesizing metal and alloy nanoparticles. This was very first technique used for synthesis of nanoparticles which involves thermal evaporation of target material in electron beam evaporation devices or Joule heated refractory crucibles at 1-50 m bar pressure. The problem associated with these techniques is non-uniform heating resulting inhomogeneous nanoparticles

1.2.9.2.7 Gamma radiation

Gamma radiation is a widely used method for metallic nanoparticles synthesis because it is reproducible, control over the shape of the particles, yields monodisperse metallic nanoparticles, simple, cheap, and use less toxins precursors: in water or solvents such as ethanol, it uses the smallest amount of reagents, it uses a reaction temperature close to room temperature with as few synthetic steps and generates small amount of by-product and waste (*Rao et al., 2010*).

1.2.9.3 Biological Method

Nanobiotechnology is an advanced field including living things of both eukaryotic and prokaryotic origin that is formed when nanotechnology and biology are combined (*Zhang et al., 2020*). This bottom-up approach used in the production of nanoparticles involves primary reactions (oxidation/reduction). These techniques use biological systems like fungus, actinomycetes, bacteria, viruses, yeast, proteins, and various plant-based extracts to produce metal and metal-oxide nanoparticles. The synthesis of nanoparticles using biological processes can be broadly divided into three categories: I) synthesis based on biomolecules; II) synthesis based on microorganisms; and III) synthesis based on plants.

1.2.9.3.1 Synthesis using microorganisms

Microorganism-based nanoparticle synthesis has garnered increased attention in recent years owing to its eco-friendliness and cost-effectiveness. Small organisms such as bacteria, fungus, and viruses are known as microbes. Microbial nanoparticles synthesis is an approach to green chemistry that blends nanotechnology and microbial biotechnology (*Narayanan and Sakthivel, 2010*).

1.2.9.3.2 Synthesis using plant extract

Plant extracts have a key role in the nanoparticles' production. This method is also known as "green synthesis" or "green nanoparticle manufacturing process" (*Mohammadzadeh et al., 2022*). Because they are cheap, spontaneous, and have a one-step biosynthetic process, plants are employed to produce nanoparticles. To create nanoparticles (NPs) with potential applications, a variety of plant extracts have been used as precursors. Quinines, flavones, and organic acids are the main water-soluble phytochemicals responsible for instant reduction. Tannic acid is a polyphenolic molecule found in various plants that can be utilized to stabilize nanoparticles

functionally, particularly gold nanoparticles (*Watcharaporn et al., 2014*). Several of plants' natural biomolecules play vital role in the formation, bio-reduction and stabilization of nanoparticles.

1.2.9.3.3 Synthesis using biomolecules

DNA, RNA, proteins, viruses, and diatoms are all strong materials that serve as templates or blueprints for the creation of nanoparticles. With a great affinity for transition metal ions, DNA is thought to be a promising option and an excellent bio-molecular template. The molecular enzyme's amino acid functional groups may serve as reducing agents during the creation of metal nanoparticles, and the remaining polypeptide chain may aid in stabilizing the nanoparticles (*Raval et al., 2007*).

1.2.10 Characterization Techniques for synthesized nanoparticles

The expansion of nanotechnology in numerous research fields has necessitated the use of analytical techniques for nanoparticles analysis and characterization. Nanoparticle characterization is a critical step in understanding the reaction mechanism and its applications. Hence, different methods and techniques are used for the analysis and characterization of the various physicochemical properties of NPs. The following analytical tools that are used to characterized synthesized nanomaterials are described in detailed.

1.2.10.1 Scanning electron microscope (SEM)

The size, shape, and surface of NPs are commonly analyzed using scanning electron microscopy (SEM). SEM offers several details about the NPs, including their size, shape, aggregation, and dispersion (*Vladár and Hodoroaba,2020*).

1.2.10.2 Transmission electron spectroscopy (TEM)

The size, shape, location, dispersity, and aggregation of NPs in two-dimensional pictures are all described by TEM. TEM can also be used to characterize the crystal structure of nanoparticles through the use of selected area electron diffraction (SAED).

1.2.10.3 Dynamic light scattering (DLS)

This technique is frequently used to analyze the size and size distribution of NPs. It uses the Strokes-Einstein equation to correlate NP velocity (diffusion coefficient) with size and measures light interference based on the Brownian motion of NPs in suspension (*Li et al., 2014*). The polydispersity index which is the result of an autocorrelation function, displays the size distribution range of NPs. The values of the polydispersity index range from 0 to 1, where 0 denotes a fully homogeneous population and 1 denotes a highly heterogeneous population.

1.2.10.4 Nanoparticle tracking analysis (NTA)

In this technique, the Brownian motion of NPs in suspensions is used to analyze their size. Size distribution profiles for NPs with diameters ranging from 10 to 1000 nm can be measured because, similar to DLS, the rate of NP movement is associated with their size using the Strokes-Einstein equation. Its advantage over DLS is that the motion of nanoparticles is analyzed using video. Compared to DLS, NTA was found to be more accurate in sizing both monodisperse and polydisperse organic NPs (*Gross et al., 2016*).

1.2.10.5 Brunauer-Emmett-Teller (BET) method

This approach is regarded as one of the best for the analysis of NP surface area and is based on the adsorption and desorption principle proposed by Edward Teller, Paul Emmett, and Stephen Brunauer (*Naderi, 2015*).

1.2.10.6 Barrett-Joyner-Halenda (BJH) method

This technique, which determines the porosity (or pore size) of NPs, is based on the Barrett–Joyner–Halenda principle. It uses N_2 gas to adsorb to the sample, just like the BET method does (*Bardestani et al., 2019*).

1.2.10.7 X-ray diffraction analysis (XRD)

This technique involves subjecting a material to incident X-ray radiation, followed by the measurement of the X-rays' intensities and scattering angles as they exit the medium (*Epp, 2016*). This method is frequently applied to the study of crystallinity and NP phase.

1.2.10.8 X-ray photoelectron spectroscopy (XPS)

This technique is thought to be the most sensitive for determining the precise elemental ratios, chemical composition, and bonding type of NP materials. The basis of XPS is the photoelectric effect, which has the high precision to identify the elements present in a material or covering a material as well as their chemical state (*Fadley, 2010*).

1.2.10.9 Fourier-transform infrared spectroscopy (FTIR)

This technique is based on exposing a material to infrared light, recording the absorbed or transmitted radiation, and analyzing the resulting spectrum, which serves as a unique fingerprint of the sample and provides information about its nature, including the bonds involved, polarity, and oxidation state (*Manor et al., 2012*).

1.2.10.10 Raman spectroscopy

This technique involves recording the interactions between a laser's light and molecular vibrations (photons and phonons) by irradiating a sample with monochromatic light. In this technique, the inelastically scattered photons, known as Raman scattering (names after the Indian physician *C. V. Raman*) is recorded. This method gives a distinct fingerprint for every sample, which is used to describe the sample's intramolecular and chemical bonding. The sample's crystallographic orientation can also be described using this technique (*Huang et al., 2009*).

1.2.10.11 Ultraviolet–visible spectroscopy (UV–vis) and photoluminescence spectroscopy

Nanomaterial research commonly makes use of UV-Vis spectroscopy, a relatively easy and affordable characterization technique. UV-vis spectroscopy makes use of both visible and UV light. The luminescence or fluorescence characteristics of a sample are measured using photoluminescence spectroscopy, which typically uses UV light to excite the electron (*Patel et al., 2020*). UV-Vis is an essential technique for characterizing, identifying, and investigating these materials as well as determining the stability of NP colloidal solution.

1.2.11 Wastewater

Wastewater refers to any water that has lost its original quality due to the presence of bacteria, microbes, organic contaminants, industrial effluent, or any other substance. It can be divided into:

- Municipal wastewater (liquid waste that is released from both residential and commercial buildings).
- Industrial wastewater (liquid waste released from agricultural and industrial processes).

1.2.11.1 Industrial paint wastewater

Paints are the most commonly utilized form of coatings. Majority of widely used paints are composed of very similar constituents such as pigments (a suspension of finely powdered materials) in a liquid medium known as a vehicle. The vehicle comprises a volatile solvent, a binder (polymeric or resinous material), and suitable additives (*Aniyikaiye, 2019*).

The paint manufacturing industry generates a lot of wastewater since it utilizes plenty of chemicals and large volume of water. Globally, the paint manufacturing industry is estimated to use between 75-85 million gallons of water each day, of which only 4% is recycled. About 25% of this effluent evaporates, and about 70% is released untreated into natural water bodies (*Nicholas, 2018*). The overall composition of wastewater from the paint industry varies greatly depending on the manufacturing operations used by particular industrial units. The direct release of these industries' effluents into water bodies leads to serious ecological instability, which includes the direct poisoning of animal biota and the impediment of aquatic plants' ability to photosynthesize (since color blocks sunlight). These impacts on the receiving streams' quality result in the depletion of dissolved oxygen (DO). Trace amounts of harmful substances in water bodies can have a negative impact on aquatic life and the food chain, among other effects on living things (*de Silva, 2016*). It

is therefore crucial to reduce their concentrations to acceptable limits before releasing them into the environment.

1.2.12 Challenges of conventional method for industrial paint wastewater treatment

Conventional wastewater treatments can be sometimes inefficient in removing certain contaminants, such as toxic heavy metals, microorganisms, and pigments from paint effluent. Also many of the current wastewater treatment methods now in use are costly and have limited abilities. Some of the pros and cons of these conventional methods in treatment of industrial wastewater is given in table 1.1 below:

Table 1.1 Pros and cons of conventional wastewater treatment methods

S/N	Treatment methods	Pros	Cons
1.	Precipitation /crystallization	i. Easy and affordable process. ii. Efficient for removing heavy metals iii. Fluoride toxicity is reduced. iv. Significant decrease in COD.	i. Consumption of chemicals. ii. pH monitoring required. iii. Ineffective at low concentrations for removing metal ions. iv. Handling and disposal problems due to large amounts of produced sludge.
2.	Coagulation /flocculation	i. Easy process ii. It is an economical process iii. Effective technique for reducing BOD and COD. iv. Capable for removing organic carbon from wastewater v. Increases sludge settling. vi. Fast and effective method for eliminating non-soluble pollutants. vii. Accessibility of numerous commercial chemicals in market as coagulant and flocculent	i. Chemicals are used as flocculants and coagulants. ii. Chemicals not reusable, leading to increased sludge volume.

3.	Flotation	i. Efficient in removing small size or low-density particles from polluted water. ii. It require less retention period and it is a selective process. iii. Useful in primary adsorption of metal and metal compounds	i. Selectivity depends on pH type. ii. High initial energy and capital costs.
4.	Biological methods	i. Inexpensive chemicals are used as it requires mainly microorganism. Microorganisms play a huge role in biodegradation of complex organic pollutant. ii. Simple and economical procedure. iii. Efficient in the removal of dark color, ammonia, iron, organic matter and complex compounds. iv. BOD and COD are also reduced.	i. Optimal growth medium and conditions like temperature and pH required. ii. Microorganism survivability and maintenance necessary. iii. Process slowed by live microorganisms. iv. Challenges with non-biodegradable dye degradation. v. Requires good understanding of microbial enzyme kinetics.
5.	Adsorption /Filtration	i. Rapid and easy method. ii. Accessibility to a wide range of commercial adsorbents. iii. Excellent ability to separate a wide range of pollutants. iv. Effective in reduction of BOD and COD demands. v. Addition of coagulation can enhance efficiency of this method for removal of suspended solids and color, Turbidity, fluoride and Suspended solids removal possible through this method	i. Non-selective and expensive method. ii. Material type significantly impacts performance. iii. Reactor saturation and clogging is common. Replacement of adsorbing material is costly.
6.	Ion exchange	i. Cost-effective method for efficiently removing metals	i. High initial costs due to resin selection for different pollutants.

		ii. Different resins can separate various types of metals and pollutants. iii. It is simple to use and maintain, iv. When combined with other techniques like precipitation and filtration, it becomes more efficient. v. Both batch and continuous operations are possible, and the process is rapid and efficient with high reusability vi. Rapid and efficient with high reusability vii. Allows for the recovery of valuable metals	ii. Long regeneration time and maintenance costs. iii. Rapid saturation and clogging issues in reactors. iv. Performance affected by pH. v. Foul smell common due to pollutants, requiring physicochemical pretreatment. vi. Matrix easily degrades in presence of strong oxidative materials.
7.	Electrochemical	i. Compared to traditional coagulation, this method is both efficient and rapid. ii. This technique enables the recovery of valuable metals such as silver, platinum, copper, and gold. iii. It enhances the biodegradability of pollutants. iv. There is no need for pH control. v. It is economically viable and highly efficient in eliminating various pollutants such as oil, suspended and dissolved solids, metals, dyes, etc.	i. High electrode cost. ii. Porous electrode maintenance and choking problems. iii. Post-treatment needed due to high metal deposition on electrodes. iv. Floc generation. v. Generated sludge adds to treatment cost.
8.	Membrane filtration	i. Chemicals are not needed. ii. Removes harmful substances such as phenols, cyanide, and zinc. iii. Wide variety of commercial membrane products are available. iv. Simple, fast, and effective even with high concentrations. v. Generates low amounts of solid waste. vi. Removes all types of dyes, salts, microorganisms,	i. High energy, maintenance, operation, and investment costs. ii. Membrane filtration systems have variable designs. iii. Membrane filter choking and fouling common. iv. Membrane selection depends on specific application.

		suspended solids, and dissolved inorganic matter. vii. Produces high-quality treated wastewater.	
9.	Ultrasonication	i. Simple to maintain. ii. Enhanced methane production with sludge pre-treatment. iii. Cost-effective pre-treatment option..	i. High cost and energy requirements ii. Ultrasonication frequency selection depends on application type. Not suitable for lignocellulosic biomass.

1.2.13 Applications of nanoparticles in wastewater treatment

The use of nanoparticles in wastewater treatment has drawn widespread attention. Advances in nanoscale science and engineering suggest that many of the current problems involving water quality could be resolved or greatly diminished by use of nanomaterials. Nanoparticles (NPs) have huge potential that enables them to participate in wastewater treatment and/or water purification technologies. Their exclusive features such as high surface area, high mechanical properties, greater chemical reactivity, lower cost and energy, enhances their adsorption capabilities (Mauter et al., 2018) and allow them to eliminate precisely toxic metal ions, viruses, bacteria, organic and inorganic solutes from the waste water (Méndez et al., 2017).

1.2.14 Commonly used nanomaterials for industrial wastewater treatment

Some of the commonly used nanomaterials are given below

- **Carbon nanotubes (CNTs)**

Carbon nanomaterials (CNMs) are intriguing materials known for their unique structures and electronic properties, making them appealing for various applications, particularly in sorption processes. Their benefits for water and wastewater treatment include a high capacity to adsorb a wide range of contaminants, rapid kinetics, large specific surface area, and selectivity towards aromatics. CNMs exist in several forms, such as carbon nanotubes (CNTs), carbon beads, carbon fibers, and nanoporous carbon, with CNTs garnering the most attention and progressing rapidly in recent years. CNTs are graphene sheets rolled up into cylinders with diameters as small as 1nm. They are highly regarded as an emerging adsorbent due to their exceptional properties. With an extremely large specific surface area and abundant porous structures, CNTs exhibit remarkable adsorption capabilities and high efficiencies for various contaminants (*Cho et al., 2010*).

- **Nanocomposite**

In recent years, there has been a notable increase in the production of various nanocomposites, which show great potential in quickly and effectively removing nitrate from water. These adsorbents have also garnered significant attention for their ability to adsorb other contaminants, such as dyes, heavy metal ions, and pesticides, from contaminated wastewater (*Rasalingam et al., 2014*) due to their large surface areas.

- **Quantum dots**

Quantum dot (QD) nanoparticles can be used for detection and removal of micro-size pollutants. QD composites are able to select and target a pollutant to remove it from sewage water. Easy and fast detection of tetrabromobisphenol pollutant and paranitrophenol pollutant from contaminated water were done with the help of Mn-doped ZnS quantum dots (*Feng et al., 2019*) and graphene quantum dots respectively (*Zhou et al., 2014*).

- **Zero-valent metal nanoparticles**

Zero-valent metal nanoparticles exhibit unique optical, mechanical, magnetic, electronic, and catalytic properties, making them valuable for remediating contaminated soils, sediments, water bodies, and wastewater. Commonly known zero-valent metal nanoparticles include zinc, silver, and iron (*Sharma et al., 2015*).

- **Metal oxide nanoparticles**

Metal oxide nanoparticles (MNPs) have emerged as a promising, environmentally friendly, and cost-effective technology for wastewater treatment. These nanoparticles have a short intraparticle diffusion distance and a high specific surface area, providing more adsorption sites and faster kinetics. Some MNPs are superparamagnetic, giving them superior adsorption performance compared to activated carbon (*Corsi et al., 2018*).

1.2.15 Mechanism of Calcium Oxide Nanoparticles in Treatment of Paint Wastewater

The treatment of paint wastewater using calcium oxide nanoparticles involves various mechanisms that contribute to the removal of contaminants from the wastewater matrix.

1.2.15.1 Adsorption Mechanism

Calcium oxide nanoparticles exhibit high surface area and reactivity, facilitating the adsorption of various contaminants present in paint wastewater (*Zhang et al., 2019*). The mechanism of adsorption involves surface interactions between the nanoparticles and pollutants, leading to their removal from the wastewater matrix.

1.2.15.2 Chemical Precipitation

CaO-NPs can induce chemical precipitation reactions with certain pollutants in paint wastewater, forming insoluble compounds that are easily removed through sedimentation or filtration (*Wang et al., 2020*). This mechanism is particularly effective for the removal of heavy metals.

1.2.15.3 pH Adjustment and Coagulation

The alkaline nature of CaO-NPs enables pH adjustment in paint wastewater, which can enhance the coagulation and flocculation of suspended solids and colloidal particles (*Huang et al., 2020*). Through coagulation mechanisms, CaO-NPs aid in the aggregation of fine particulates, facilitating their removal by sedimentation or filtration processes.

1.2.15.4 Oxidation and Degradation

CaO-NPs possess oxidizing properties that promote the degradation of organic pollutants present in paint wastewater (*Jiang et al., 2021*). Through oxidative reactions, these nanoparticles facilitate the breakdown of complex organic molecules into simpler, less harmful compounds, enhancing treatment efficiency.

CHAPTER TWO

MATERIAL AND METHODOLOGY

2.1 Materials and Reagent.

2.1.1 Collection of materials

Waste snail shells (*Archachatina marginata* shells) were locally sourced from uselu market in Benin City, Edo State. The paint wastewater was collected from Motion Paint and

Decoration company located at PLOT 5/4 Omokhalen street, off Federal Government Girls College Rd, Benin City.

2.1.2 List of Reagents

- 1M Sodium hydroxide (NaOH)
- 1M Hydrochloric acid (HCl)
- Deionized water

2.1.3 Equipment and apparatus

Glassware utilized in the experiments includes conical flasks, beakers of different volume, measuring cylinders of various sizes, separating funnels, stirring rod. The equipment utilized in the experiments are shown below in Table 2.1

Table 2.1: List of equipment and their model/manufacturer

Equipment	Model/ Manufacturer
Magnetic stirrer	MSH-30A/ Witeg Labortechnik GmbH England
Centrifuge	BKC-TH18II/ JINAN BIOBASE Medical Co., LTD. China
Muffle furnace	Thermolyne 480000/ Thermo Fisher Scientific

Weighing Balance	AV264/ OHAUS Adventurer Pro Analytical balance
Grinding mill machine	Grinding mill with GX-390 petrol engine
Oven	I475-2 large vacuum oven/ Shel Lab
pH meter	PHS-3C pH meter/ Puchun Co., LTD
Cycling Vibrator	HY-4A Cycling Vibrator/ Wincom Company Ltd.
XRD machine	RU-200BH X-ray diffractometer/ Rigaku
FTIR machine	FTIR-8400S/ Shimadzu, Japan
DLS machine	ZEN-16000/ MALVERN instrument LTD.
UV-VIS Spectrophotometer	UV-6300PC double beam spectrophotometer/ VWR

2.2. Methods

2.2.1 Sample preparation and pretreatment

The waste snail shells obtained was first washed thoroughly with tap water to remove dust, impurities, and organic matters adhered on the surface of the snail shells, then cleaned with deionized water several times. The thoroughly washed snail shells were dried in an oven at 150°C for 3hr to remove water. The dried snail shells were ground by a grinding mill machine into a fine powder. The fine snail shell powder was passed through a sieve mesh of 100µm to obtain the finest snail shell powder. The obtained snail shell powder was placed in a sealed plastic container.

Fig. 2.1 Snail shells before cleaning

Fig. 2.2 Snail shells after cleaning

Fig 2.3 Powdered snail shells

2.2.2 Preparation of reagents

2.2.2.1 Preparation of 1M HCl solution

1000 mL of 1M hydrochloric acid (HCl) solution was prepared via the following the following steps:

83.33 mL of concentrated hydrochloric acid (37% HCl) was measured using a graduated cylinder. The measured HCl was transferred to a 1000 mL volumetric flask using a funnel. Deionized water was added to the flask up to the mark (1000 mL). The solution was mixed thoroughly using a magnetic stirrer. The resulting solution is a 1M HCl solution, which was used in the experimental procedures.

2.2.2.2 Preparation of 1M NaOH Solution

1000 mL of 1 M sodium hydroxide (NaOH) solution was prepared via the following steps:

40.00 g of sodium hydroxide (NaOH) pellets was measured using a balance. The measured NaOH pellets was transferred into a 1000 mL volumetric flask. Deionized water was added to the flask up to the mark (1000 mL). The solution was mixed thoroughly by swirling the flask gently until all the NaOH pellets are dissolved. The resulting solution is a 1M NaOH solution, which was used in the experimental procedures.

2.2.3 Synthesis of Calcium Oxide Nanoparticles

Calcium oxide nanoparticles were synthesized from powdered snail shells using the sol-gel method via the following procedures:

The first step involved the preparation of metallic salt ($CaCl_2$), by dissolving the powdered snail shell in hydrochloric acid. 50g of the sieved powder snail shells (PSS) was measured and dissolved in 1000ml of 1M hydrochloric acid (HCl) as shown in Fig 2.4. The mixture was stirred

continuously at room temperature for 1hr using a magnetic stirrer to ensure complete dissolution of the $CaCO_3$ as shown in Fig 2.5

$$PSS/CaCO_3(s) + 2HCl(aq) \rightarrow CaCl_2(aq) + H_2O\ (l) + CO_2(g) \qquad (2.1)$$

Fig. 2.4: Powdered snail shell dissolved in HCl

Fig. 2.5: Complete dissolution of the powdered snail shell in HCl

Next, the solution was filtered using a filter paper to separate the $CaCl_2$ solution from any undissolved residue. Then the filtered $CaCl_2$ solution was transferred into a clean beaker as shown in Fig. 2.6

Fig. 2.6: $CaCl_2$ filtrate

The next step involved the formation of sol by hydrolysis reaction. During the hydrolysis process, metal hydroxide was formed. A total of 1000ml of 1M sodium hydroxide (NaOH) was added slowly (drop by drop) with continuous stirring on a magnetic stirrer to convert the homogeneous $CaCl_2$ solution formed in the previous step into 'sol' at ambient temperature, equation (2.2) and the pH of the solution was tested.

$$CaCl_2(aq) + 2NaOH\ (aq) \rightarrow Ca(OH)_2(s) + 2NaCl\ (aq) \qquad (2.2)$$

Next, the gel was generated by a condensation reaction. The slow addition of NaOH resulted in a low rate of nucleation and encouraged subsequent precipitation of $Ca(OH)_2$ one over another forming a highly crystalline gel as shown in Fig.2.7

$Ca(OH)_2$ gel containing solution was aged for one night at room temperature, and the $Ca(OH)_2$ precipitate formed was allowed to settle (Fig 2.8) and then the supernatant liquid was decanted to separate it from the solid precipitate. The remaining $Ca(OH)_2$ precipitate was transferred to a centrifuge tube and placed in the centrifuge machine at 10,000rpm for 5min

Fig. 2.7: $Ca(OH)_2$ precipitate

After centrifugation, the supernatant (liquid) was carefully removed, leaving behind the solid $Ca(OH)_2$ precipitate. The precipitate was then washed several times with deionized water to remove any impurities or residual reactants and transferred into a crucible (Fig. 2.9). The washing process helped to ensure the purity of the final product.

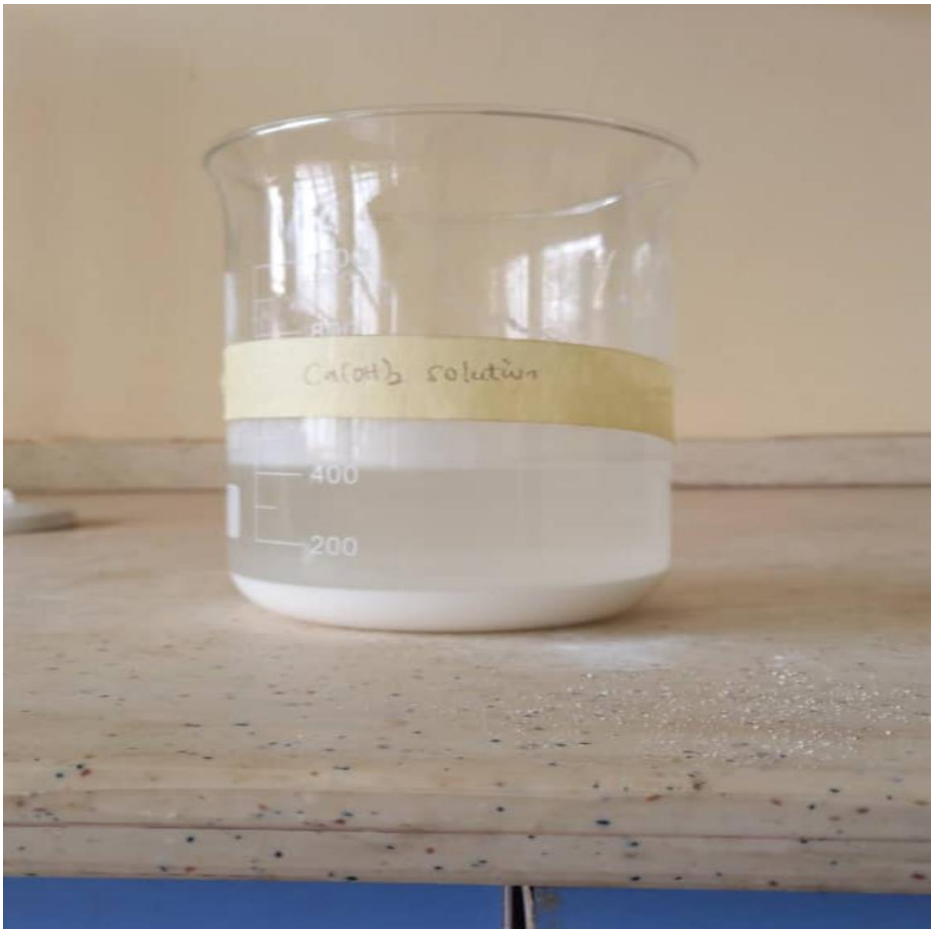

Fig. 2.8: $Ca(OH)_2$ solution after standing overnight

Finally, water was removed from the generated gel by drying at 100°C for 3hrs in an oven and the dried $Ca(OH)_2$ and calcined at 900°C for 1hr in a muffle furnace to obtain Calcium Oxide nanoparticles (Fig.2.10)

$$Ca(OH)_2(s) + Heat \rightarrow CaO(s) + H_2O(l) \qquad (2.3)$$

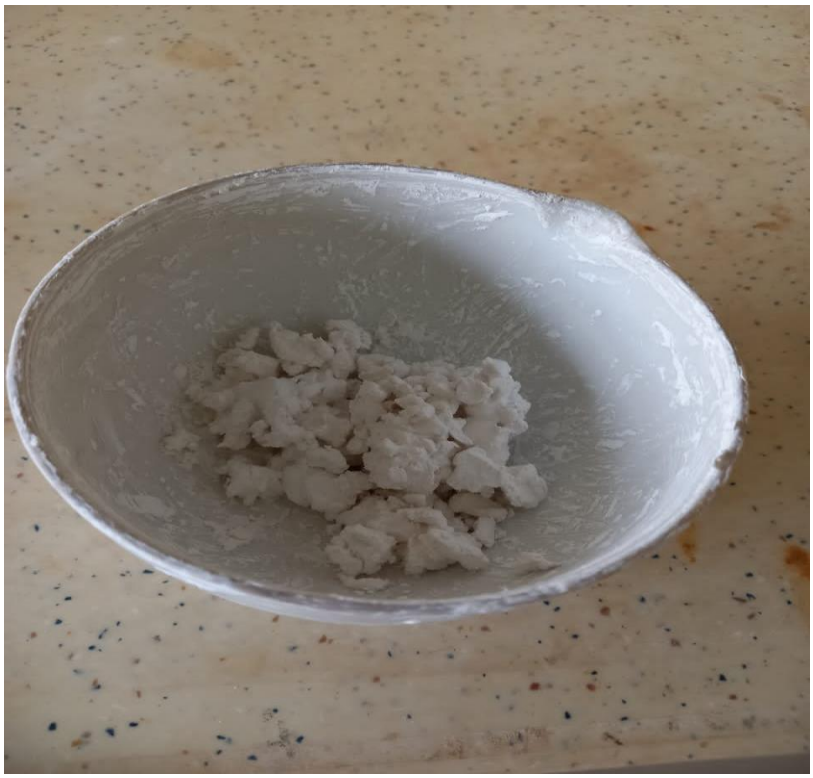

Fig. 2.9: Solid $Ca(OH)_2$ sample formed

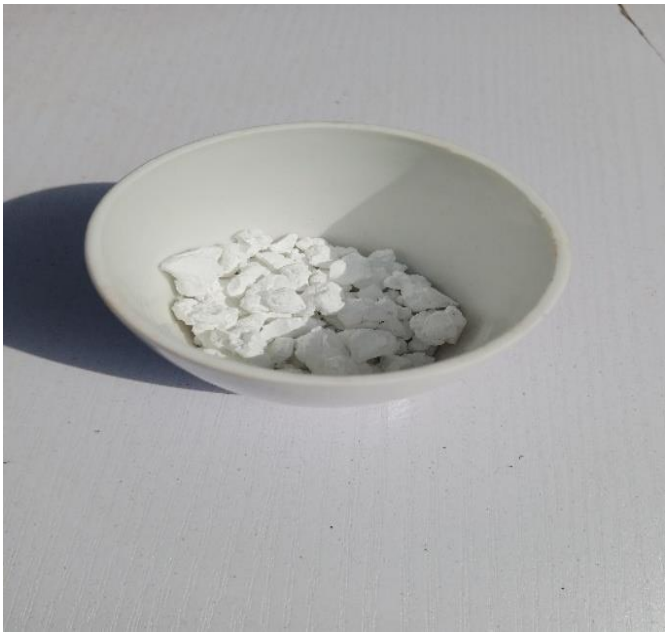

Fig. 2.10: Synthesized CaO nanoparticles

The synthesized CaO nanoparticles was powdered using mortal and pestle and transferred into a clean sealed container (fig 2.11)

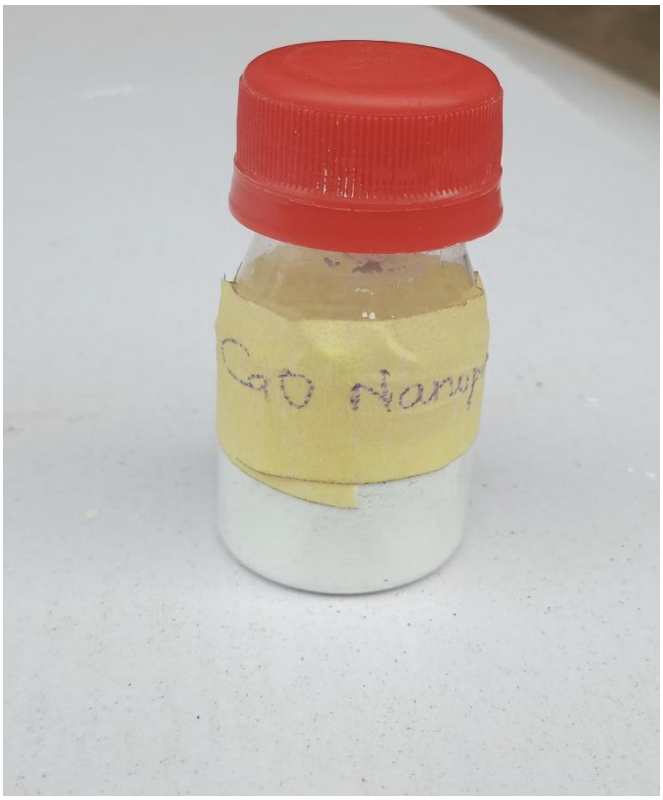

Fig. 2.11: Synthesized CaO nanoparticles after grinding

2.2.4 Characterization of Calcium oxide nanoparticles

The synthesized CaO nanoparticles were characterized using various analytical techniques to determine their structural and chemical properties.

2.2.4.1 X-ray Diffraction (XRD) Analysis

X-ray diffraction (XRD) analysis was performed to investigate the crystal structure of the synthesized CaO nanoparticles. The XRD patterns were recorded in the 2θ range.

2.2.4.2 Dynamic Light Scattering (DLS) Analysis

Dynamic light scattering (DLS) was utilized to determine the size distribution of the synthesized CaO nanoparticles in solution. A Malvern Zetasizer Nano ZS instrument was employed for the DLS measurements. Prior to analysis, the nanoparticles were dispersed in deionized water and sonicated to ensure uniform dispersion. The hydrodynamic diameter of the nanoparticles was measured at room temperature, and the results were analyzed to determine the size distribution profile.

2.2.4.3 Fourier Transform Infrared (FTIR) Spectroscopy

Fourier transform infrared (FTIR) spectroscopy was used to analyze the functional groups present in the synthesized CaO nanoparticles. To prepare the sample for analysis, the CaO nanoparticles were ground with potassium bromide (KBr) and compressed into a thin pellet. The spectra were recorded and analyzed to identify the characteristic absorption bands corresponding to various functional groups present on the surface of the nanoparticles.

2.2.4.4 Scanning Electron Microscopy (SEM)

Scanning Electron Microscopy (SEM) was employed to analyze the morphology and structure of the synthesized calcium oxide (CaO) nanoparticles. The SEM analysis provides high-resolution images, allowing for the observation of particle size, shape, and surface morphology. SEM images were captured at various magnifications (1000×, 500×, and 2000×) to provide a detailed view of the nanoparticles. The images were analyzed to determine the size distribution and morphology of the nanoparticles, providing valuable insights into their structural properties.

2.2.5 Paint wastewater sample preparation

Industrial paint wastewater samples were collected from a paint manufacturing plant in accordance with environmental regulations. The samples were stored in clean, labeled containers at 4°C to prevent microbial growth and chemical degradation.

Fig. 2.12: Industrial paint wastewater samples

2.2.6 Characterization of Untreated Paint Wastewater

The untreated paint wastewater samples were characterized for pH, total dissolved solids (TDS) and electrical conductivity (EC).

2.2.7 Optimization of Treatment Conditions

2.2.7.1 Selection of Factors

The factors considered for optimization were pH, contact time, and adsorbent dosage, as they play crucial roles in the adsorption process.

pH: The pH of the paint wastewater was adjusted using 1M HCl or 0.25M NaOH to determine its effect on the adsorption efficiency of CaO nanoparticles.

Contact Time: The contact time between the CaO nanoparticles and paint wastewater was varied to determine the optimum contact time for maximum Adsorption efficiency.

Adsorbent Dosage: The amount of CaO nanoparticles added to the paint wastewater was varied to determine the optimum dosage for maximum adsorption efficiency.

2.2.7.2 Experimental Design using Central Composite Design (CCD)

RSM with CCD was employed to design the experiments and analyze the response surface. This design allows for the determination of quadratic effects and interactions between factors.

Factorial Points: The experimental design included a set of factorial points at different levels of pH, contact time, and adsorbent dosage.

Center Points: Center points were included in the design to estimate the experimental error and check the adequacy of the model.

Axial Points: Axial points were included to estimate the curvature of the response surface.

Table 2.2: Build Information

File Version	13.0.1.0
Study Type	Response Surface
Design Type	Central Composite
Design Model	Quadratic
Build Time (ms)	4.00
Subtype	Randomized
Runs	20.00
Blocks	No Blocks

Table 2.3: Design Factors

Factor Name	Units	Mini	Coded Low	Mean	Coded High	Max	Std. Dev.
A: Adsorbent dosage	g/L	1.0000	2.82	5.50	8.18	10.00	2.27
B: Time	minutes	15.00	30.20	52.50	74.80	90.00	18.90
C: pH	-	4.00	5.22	7.00	8.78	10.00	1.51

2.2.8 Experimental set-up

A total of 20 experimental runs were conducted according to the CCD matrix, including 4 replicates at the center point to estimate the experimental error. Each experimental run was conducted by varying the pH (X1), contact time (X2), and adsorbent dosage (X3) according to the CCD matrix.

Batch adsorption experiments were set for performing all experiments. All experiments were conducted in a conical flask of 250mL capacity. In each experiment, the volume of the paint wastewater sample used was 50mL. The pH of the wastewater was adjusted to the desired level using 1M HCl or 0.25M NaOH. A predetermined amount of CaO nanoparticles was added to the wastewater. The mixture was agitated using a cycling vibrator at 150 rpm for the specified contact time. After agitation, the mixture was filtered using filter papers and the filtrate was analyzed by a UV-VIS spectrophotometer at 540nm to determine the removal efficiency of contaminants. The experimental run was repeated for each combination of pH, contact time, and adsorbent dosage according to the CCD matrix.

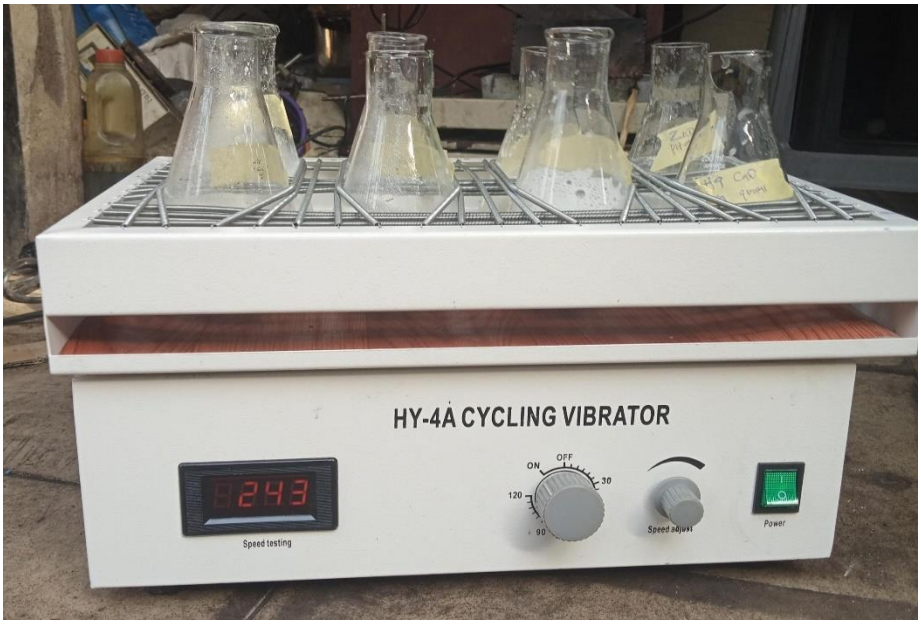

Fig. 2.13: Experimental set-up for the treatment process

Fig 2.14: Industrial paint wastewater samples after treatment

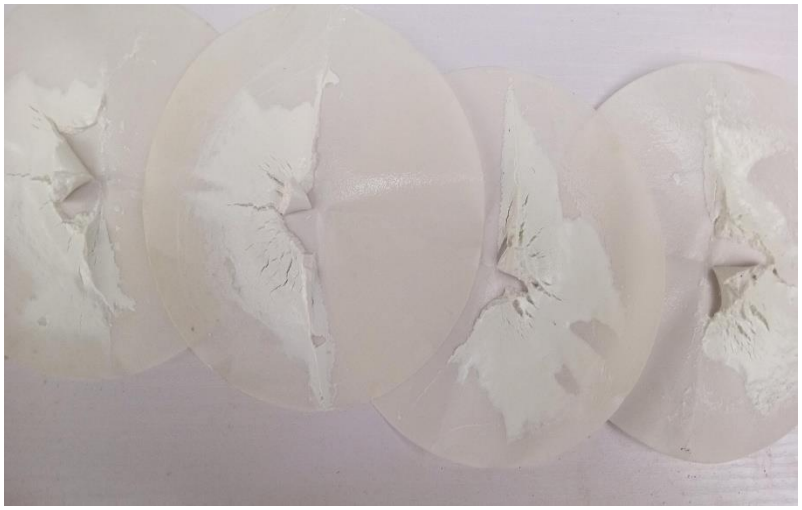

Fig. 2.15: Residues obtained after treatment and filtration of the paint wastewater

2.2.9 Data Collection:

Data on the removal efficiency of paint wastewater contaminants by CaO nanoparticles were collected for each experimental run.

2.2.10 Data Analysis:

The data obtained from the experiments were analyzed statistically using Design-Expert software to determine the optimum conditions for maximum removal efficiency.

Model Fitting: The data obtained from the experiments were used to fit a second-order polynomial model using Design-Expert software.

ANOVA: Analysis of Variance (ANOVA) was performed to assess the significance of the model and the factors.

Model Validation: The validity of the model was checked by comparing the predicted values with the experimental results obtained under the optimized conditions.

2.2.10.1 Response Variable

The removal efficiency of paint wastewater contaminants by CaO nanoparticles was calculated based on the initial and final concentrations of contaminants.

2.2.10.2 Model Validation

The validity of the model was checked by comparing the predicted values with the experimental results obtained under the optimized conditions.

2.2.10.3Analysis of Response Surface

The response surface plots were analyzed to visualize the effects of the factors and their interactions on the response variable.

2.2.10.4 Optimization Algorithm

The optimization algorithm in Design-Expert software was used to find the optimum conditions for maximum removal efficiency.

2.11 Confirmation Experiment

A confirmation experiment was conducted under the predicted optimum conditions to validate the optimization results.

CHAPTER THREE

RESULTS AND CONCLUSION

3.1 Characterization of adsorbent

3.1.1 Fourier Transform Infrared (FTIR) Spectroscopy

Fourier Transform Infrared (FTIR) spectroscopy was employed to analyze the functional groups present in the CaO nanoparticles synthesized from snail shells using the sol-gel method. The FTIR spectrum exhibited three distinct peaks at 3641.6 cm^{-1}, 1408.9 cm^{-1}, and 875.9 cm^{-1}, as seen in Fig. 3.1, which are indicative of specific functional groups.

The peak at 3641.6 cm^{-1} corresponds to the stretching vibration of hydroxyl (OH) groups. These OH groups likely originate from the surface hydroxylation of the nanoparticles during the sol-gel process. The use of NaOH in the synthesis process likely contributes to the surface hydroxylation of the nanoparticles, as NaOH can generate hydroxide ions (OH^-) that react with dissolved calcium ions to form calcium hydroxide ($Ca(OH)_2$). The presence of hydroxyl groups may also suggests that some residual moisture may still be present on the nanoparticle surface.

The peak at 1408.9 cm^{-1} is attributed to the bending vibration of carbonate (CO_3^{2-}) ions. This peak is consistent with the use of snail shells as the precursor material, as snail shells are predominantly composed of calcium carbonate. The presence of carbonate groups on the surface of the CaO nanoparticles indicates that some carbonate residues may have remained after the calcination process or that some carbon dioxide (CO_2) from the atmosphere has been absorbed onto the nanoparticle surface.

The peak at 875.9 cm^{-1} is associated with the stretching vibration of carbonate (CO_3^{2-}) ions. This peak further confirms the presence of carbonate groups on the nanoparticle surface, providing additional evidence of the retention of carbonate residues from the snail shells. The presence of carbonate peaks can also be attributed to the adsorption of carbon dioxide (CO_2) from the atmosphere onto the nanoparticle surface. This adsorbed CO_2 can react with surface hydroxyl groups to form carbonate ions.

The FTIR analysis confirms the successful synthesis of CaO nanoparticles from snail shells using the sol-gel method and provides insights into the chemical composition and surface functional groups present in the nanoparticles.

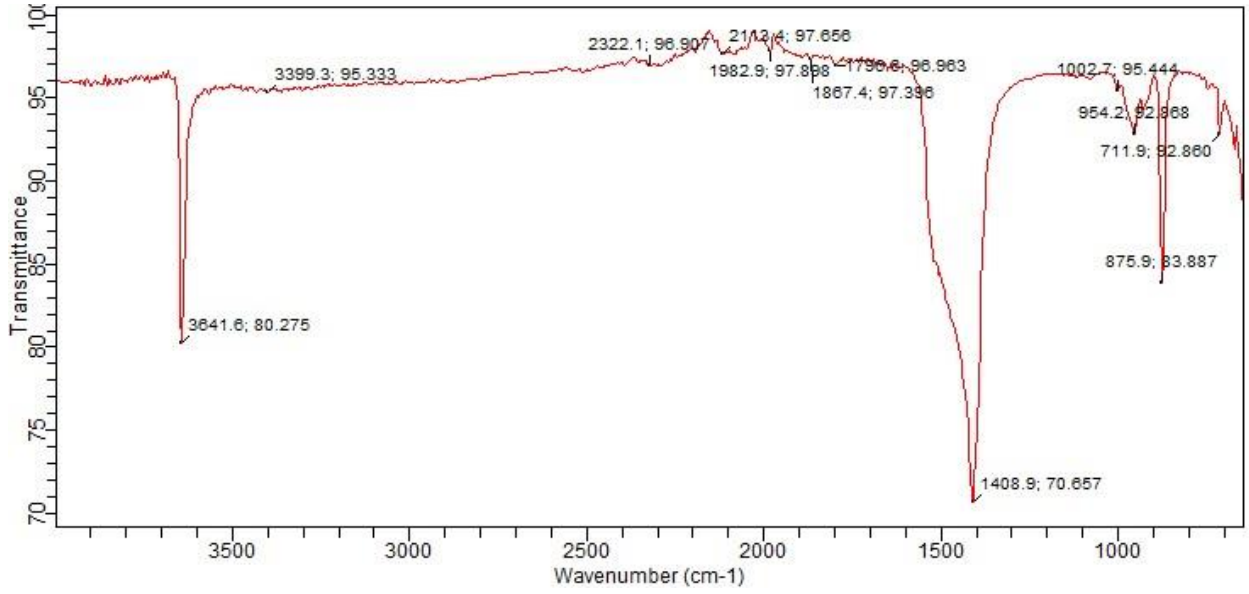

Fig 3.1: Fourier Transform Spectroscopy of CaO nanoparticles synthesized from snail shells

Table 3.1: Wavenumber and their corresponding functional groups in FTIR spectrum of CaO nanoparticles synthesized from snail shells

Wave Number (cm^{-1})	Functional Group	Peak Assignment
3641.6	Hydroxyl (OH)	O-H stretching
1408.9	Carbonate (CO_3^{2-})	Bending vibration belonging to carbonate functional group
875.9	Carbonate (CO_3^{2-})	Stretching vibration belonging to carbonate functional group

3.1.2 Dynamic Light Scattering (DLS) Analysis

Dynamic Light Scattering (DLS) analysis was conducted to determine the size distribution of the synthesized CaO nanoparticles. DLS measures the intensity of scattered light caused by the Brownian motion of nanoparticles in solution, allowing for the calculation of their hydrodynamic diameter. The analysis revealed the following key results:

The size Distribution Report by Intensity shown in Fig. 3.2 showed the size distribution of particles based on the intensity of scattered light. It showed three distinct peaks. Peak 1 had a diameter of 103.4 nm with an intensity of 76%, indicating that a large proportion of the scattered light was from particles of this size. Peak 2 had a diameter of 2.319 nm with an intensity of 13%, and Peak

3 had a diameter of 1471 nm with an intensity of 5.7%. The presence of multiple peaks suggests a polydisperse system with particles of varying sizes.

The size distribution report by volume shown in Fig. 3.3 provides a more accurate representation of the size distribution, taking into account the volume of particles. The Z-average value, which represents the mean diameter of the particles, was measured to be 46.12 nm. The polydispersity index (PDI), a measure of the width of the size distribution, with values greater than 0.05 indicating polydispersity and values less than 0.05 indicating monodispersity. In this case, the PDI value of 0.488 confirms the polydispersed nature of the nanoparticles.

The size Quality Report Fig. 3.4 evaluates the quality of the size distribution data. It provides information about how well the data obtained from the DLS experiment fits the theoretical models used to analyze the scattering pattern and calculate the particle size distribution. The size quality result can either be good or poor. A good size quality report indicates that the data is reliable and the measured particle sizes are likely accurate as seen in fig as there is a good fit to the cumulant data

The correlogram Fig. 3.5 is a plot showing the autocorrelation function of the scattered light intensity. It provides information about the dynamics of particle motion in solution and can be used to determine the diffusion coefficient of the nanoparticles. The slope in the correlogram also shows that the nanoparticle is polydispersed.

The cumulant fit analysis Fig. 3.6 is used to extract the mean size and PDI of the nanoparticles. The PDI value of 0.488 suggests a relatively broad size distribution (the particles vary significantly in size, resulting in a wide range of particle sizes within the sample).

The distribution fit report Fig. 3.7 compares the experimental data with theoretical distribution models such as the Gaussian distributions. This helps determine the best-fit model for describing the size distribution of the nanoparticles.

Size Distribution Report by Number Fig. 3.8 shows the size distribution of particles based on the number of particles. It provides information about the particle concentration at each size range. Overall, the DLS analysis provides comprehensive information about the size distribution and quality of the synthesized CaO nanoparticles, essential for understanding their behavior and potential applications in wastewater treatment.

Sample Details

Sample Name:	CaO NP
SOP Name:	Abdulrahman.sop
General Notes:	Average result created from record number(s): 3917 3924

File Name:	D L S.dts	**Dispersant Name:**	Water
Record Number:	3931	**Dispersant RI:**	1.330
Material RI:	1.59	**Viscosity (cP):**	0.8872
Material Absorbtion:	0.010	**Measurement Date and Time:**	23 April 2024 12:29:56

System

Temperature (°C):	25.0	**Duration Used (s):**	70
Count Rate (kcps):	206.0	**Measurement Position (mm):**	4.65
Cell Description:	Disposable sizing cuvette	**Attenuator:**	8

Results

			Size (d.n...	% Intensity:	St Dev (d.n...
Z-Average (d.nm):	46.12	**Peak 1:**	102.4	76.0	141.3
PdI:	0.488	**Peak 2:**	2.319	13.0	1.606
Intercept:	0.270	**Peak 3:**	1471	5.7	483.2
Result quality	Good				

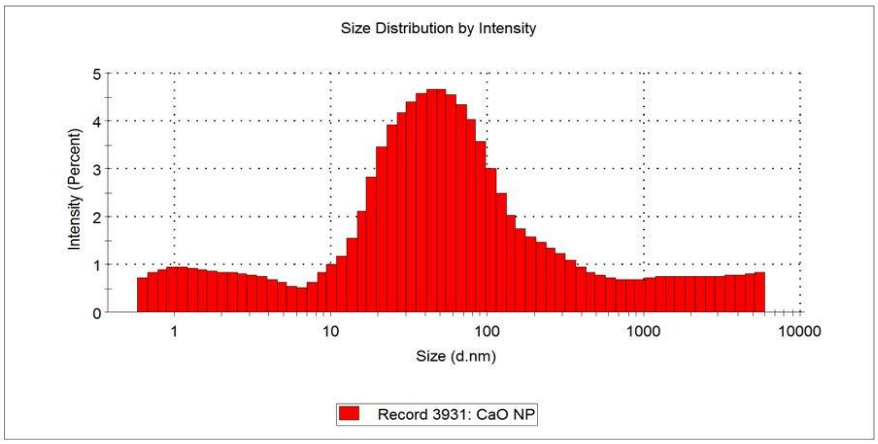

Fig. 3.2: Size distribution report by Intensity

Sample Details

Sample Name:	CaO NP		
SOP Name:	Abdulrahman.sop		
General Notes:	Average result created from record number(s): 3917 3924		
File Name:	D L S.dts	**Dispersant Name:**	Water
Record Number:	3931	**Dispersant RI:**	1.330
Material RI:	1.59	**Viscosity (cP):**	0.8872
Material Absorbtion:	0.010	**Measurement Date and Time:**	23 April 2024 12:29:56

System

Temperature (°C):	25.0	**Duration Used (s):**	70
Count Rate (kcps):	206.0	**Measurement Position (mm):**	4.65
Cell Description:	Disposable sizing cuvette	**Attenuator:**	8

Results

			Size (d.n...	% Volume:	St Dev (d.n...
Z-Average (d.nm):	46.12	**Peak 1:**	17.81	32.6	6.358
PdI:	0.488	**Peak 2:**	0.8823	35.3	0.4041
Intercept:	0.270	**Peak 3:**	73.05	31.7	110.7
Result quality	Good				

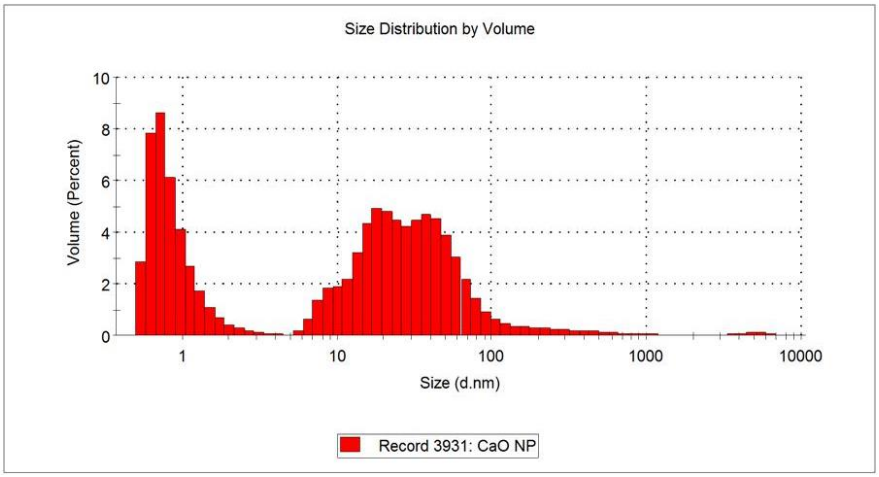

Fig. 3.3: Size distribution report by volume

Sample Details

Sample Name:	CaO NP		
SOP Name:	Abdulrahman.sop		
General Notes:	Average result created from record number(s): 3917 3924		
File Name:	D L S.dts	**Dispersant Name:**	Water
Record Number:	3931	**Dispersant RI:**	1.330
Material RI:	1.59	**Viscosity (cP):**	0.8872
Material Absorbtion:	0.010	**Measurement Date and Time:**	23 April 2024 12:29:56

System

Temperature (°C):	25.0	**Duration Used (s):**	70
Count Rate (kcps):	206.0	**Measurement Position (mm):**	4.65
Cell Description:	Disposable sizing cuvette	**Attenuator:**	8

Results

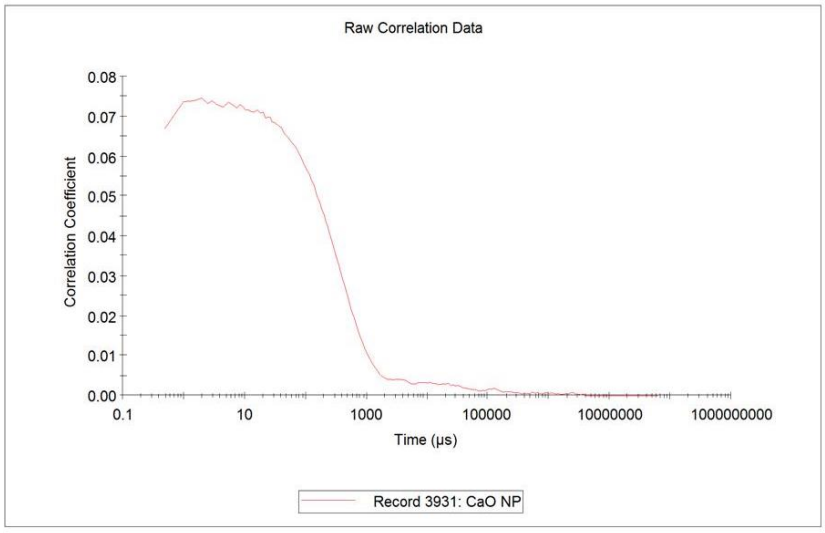

Fig. 3.4: Correlogram report

Sample Details

Sample Name: CaO NP
SOP Name: Abdulrahman.sop
General Notes: Average result created from record number(s): 3917 3924

File Name:	D L S.dts	**Dispersant Name:**	Water
Record Number:	3931	**Dispersant RI:**	1.330
Material RI:	1.59	**Viscosity (cP):**	0.8872
Material Absorbtion:	0.010	**Measurement Date:**	23 April 2024 12:29:56

System

Temperature (°C):	25.0	**Duration Used (s):**	70
Count Rate (kcps):	206.0	**Measurement Position (mm):**	4.65
Derived Count Rate (kcps):	4682.3	**Attenuator:**	8
Cell Description:	Disposable sizing cuvette		

Results

Cumulants Fit Error: 7.67e-4

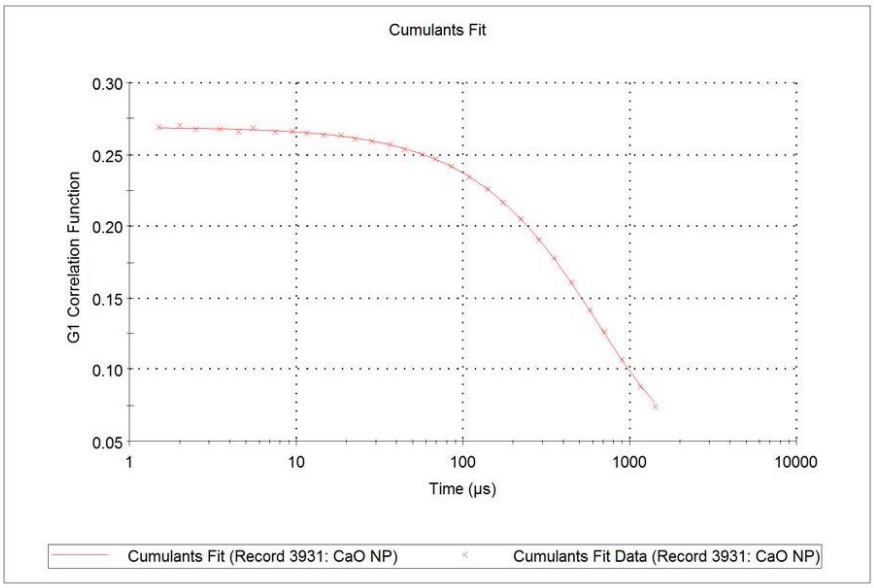

Fig. 3.5: Cumulants fit report

Sample Details

Sample Name:	CaO NP
SOP Name:	Abdulrahman.sop
General Notes:	Average result created from record number(s): 3917 3924

File Name:	D L S.dts	**Dispersant Name:**	Water
Record Number:	3931	**Dispersant RI:**	1.330
Material RI:	1.59	**Viscosity (cP):**	0.8872
Material Absorbtion:	0.010	**Measurement Date and Time:**	23 April 2024 12:29:56

System

Temperature (°C):	25.0	**Duration Used (s):**	70
Count Rate (kcps):	206.0	**Measurement Position (mm):**	4.65
Derived Count Rate (kcps):	4682.3	**Attenuator:**	8
Cell Description:	Disposable sizing cuvette		

Results

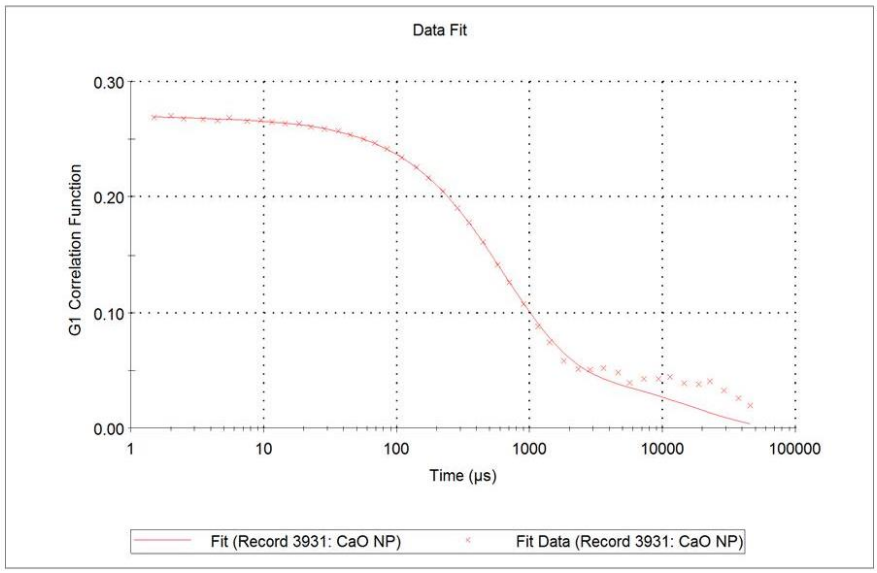

Fig. 3.6: Distribution fit report

Sample Details

Sample Name: CaO NP
SOP Name: Abdulrahman.sop
General Notes: Average result created from record number(s): 3917 3924

File Name:	D L S.dts	**Dispersant Name:**	Water
Record Number:	3931	**Dispersant RI:**	1.330
Material RI:	1.59	**Viscosity (cP):**	0.8872
Material Absorbtion:	0.010	**Measurement Date and Time:**	23 April 2024 12:29:56

System

Temperature (°C):	25.0	**Duration Used (s):**	70
Count Rate (kcps):	206.0	**Measurement Position (mm):**	4.65
Cell Description:	Disposable sizing cuvette	**Attenuator:**	8

Results

			Size (d.n...	% Number:	St Dev (d.n...
Z-Average (d.nm):	46.12	**Peak 1:**	0.7151	34.7	0.1663
PdI:	0.488	**Peak 2:**	3.950	0.0	0.5957
Intercept:	0.270	**Peak 3:**	8.195	7.7	1.360

Result quality Good

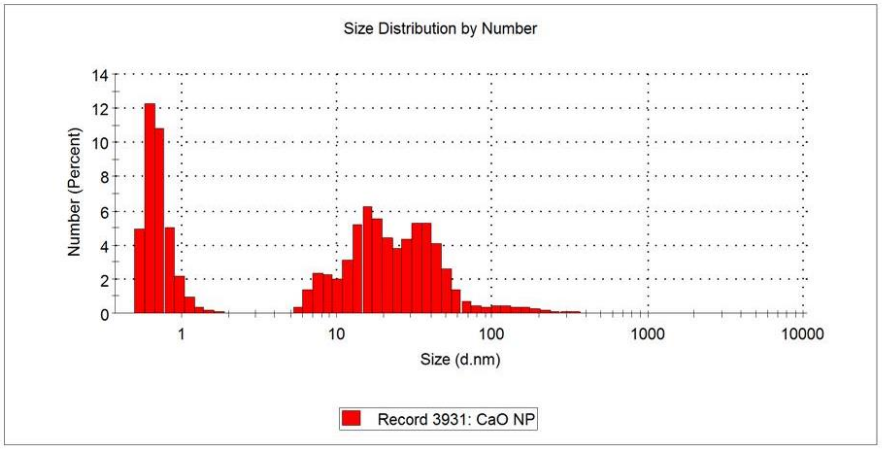

Fig. 3.7: Size distribution report by number

Sample Details

Sample Name:	CaO NP
File Name:	D L S.dts
SOP Name:	Abdulrahman.sop
General Notes:	Average result created from record number(s): 3917 3924

Measurement Date and Time:	April 23, 2024 12:29:56		
Cell Description:	Disposable sizing cuvette		
Temperature (°C):	25.00139		
Dispersant Name:	Water		
Dispersant RI:	1.330	**Material RI:**	1.590
Viscosity (cP):	0.8872	**Material Absorption:**	0.010

Results

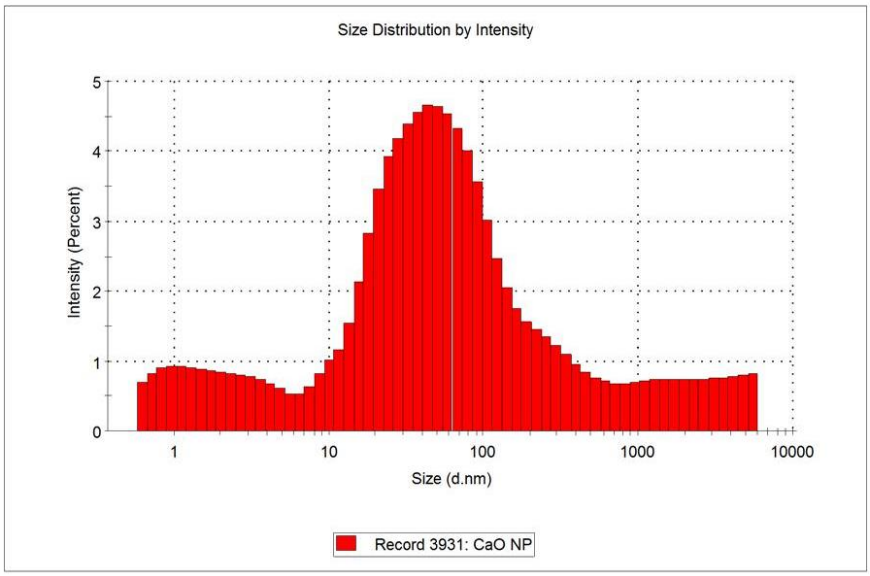

Fig. 3.8: Size distribution overlay report by intensity

3.1.3 X-ray Diffraction (XRD) Analysis

X-ray Diffraction (XRD) analysis was performed to determine whether the synthesized sample was CaO NPs or not and to investigate the crystal structure and purity of the synthesized nanoparticles. The XRD pattern shown in Fig. 3.9 exhibited three distinct peaks at 2θ values of 33.9°, 37.2°, and 53.7°, corresponding to the (101), (102), (004), and (110) crystallographic planes of calcium oxide (CaO), respectively.

The presence of these peaks confirms the formation of crystalline CaO nanoparticles. The peak positions are in good agreement with the standard reference pattern for CaO (JCPDS card no. 75-0449), indicating the phase purity of the synthesized nanoparticles

The sharpness of the peaks as seen in Fig. 3.9 showed a high degree of crystallinity of the synthesized CaO nanoparticles. The XRD analysis also provided information about the phase composition of the sample, as shown in Fig. 3.10. These results indicate that the majority (76.7%) of the sample consists of Lime (CaO), which is the desired product of the synthesis.

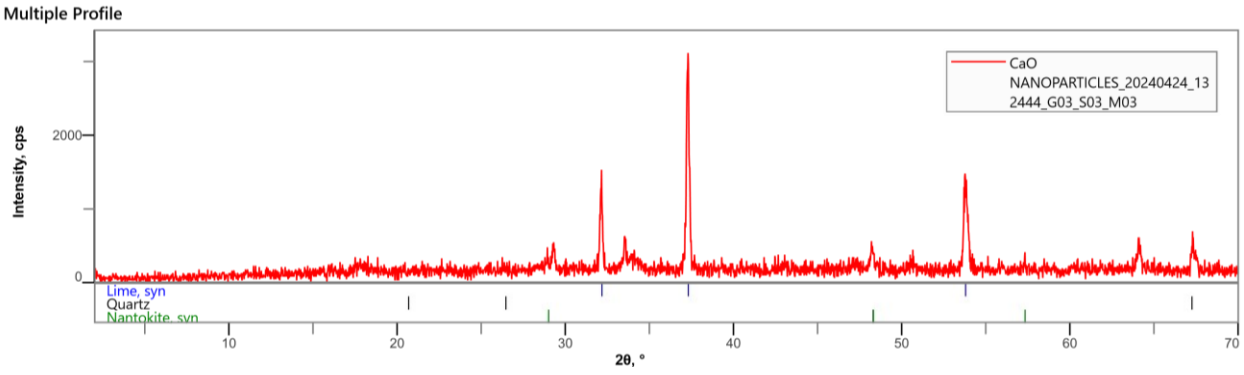

Fig. 3.9: XRD image of CaO nanoparticles synthesized from snail shells

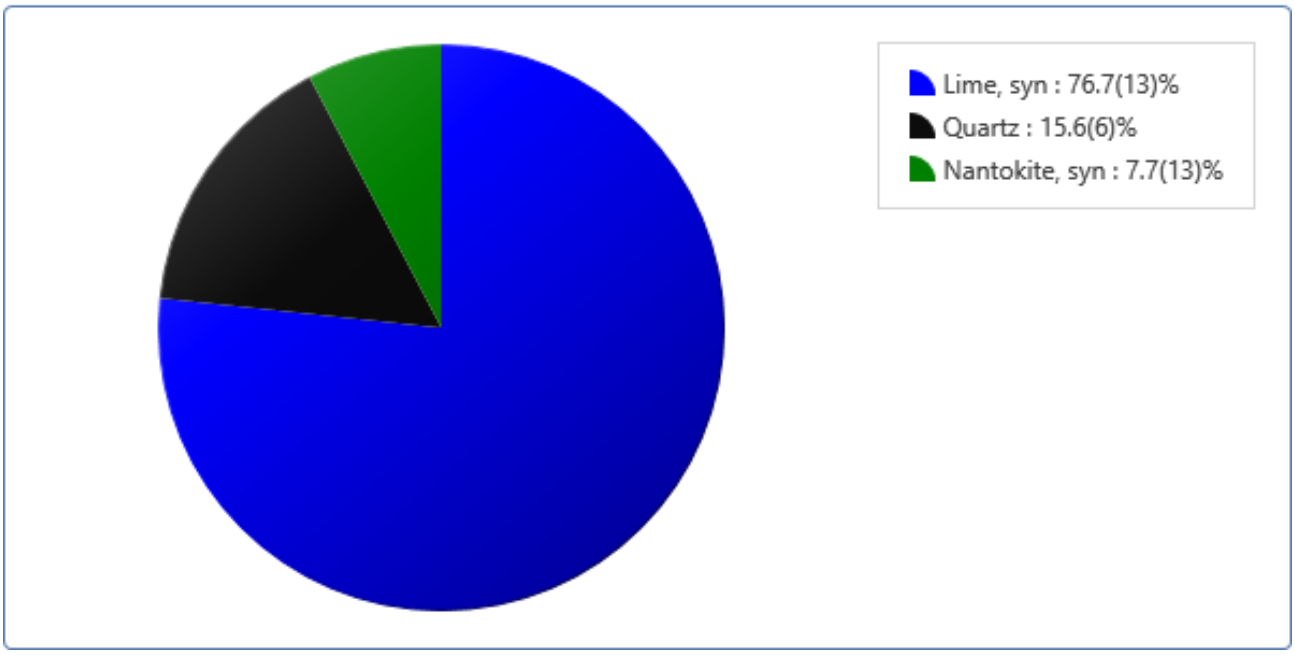

Fig. 3.10: Pie chart of the phase composition of the synthesized CaO nanoparticles

3.1.4 Scanning Electron Microscopy (SEM)

Scanning electron microscopy (SEM) was employed to investigate the morphology and surface structure of the synthesized CaO nanoparticles (CaO-NPs) derived from snail shells. The SEM analysis provided valuable insights into the physical characteristics of the nanoparticles, enhancing our understanding of their potential applications in wastewater treatment.

The SEM images revealed that the CaO-NPs exhibited a spherical morphology. The nanoparticles appeared to be agglomerated, forming larger clusters with irregular shapes. The surface of the nanoparticles exhibited roughness and porosity, which could enhance their adsorption capacity and facilitate interactions with contaminants in wastewater. These findings further support the suitability of CaO-NPs as an adsorbent for contaminants removal in industrial effluent treatment applications.

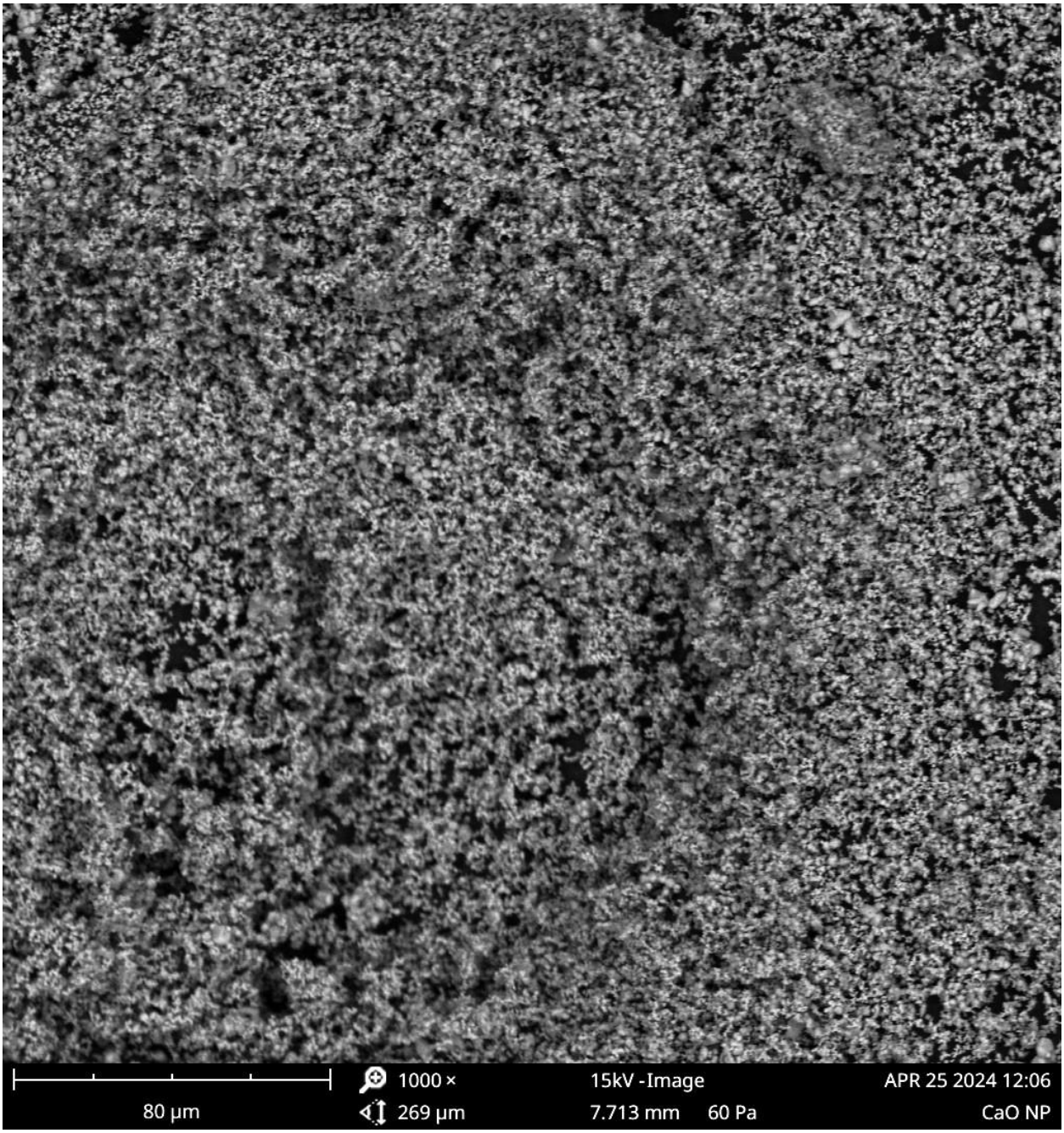

Fig 3.11: SEM Image of CaO-NPs

3.2 Optimization of Treatment of Paint Wastewater

The treatment of paint wastewater was optimized using Response Surface Methodology (RSM) with Central Composite Design (CCD). The optimization aimed to determine the optimal conditions for pH, contact time, and adsorbent dosage to maximize the adsorption efficiency of the CaO nanoparticles.

3.2.1 Experimental Design

A Central Composite Design (CCD) was used to design the experiments for optimizing the treatment process. The design included a set of factorial points, axial points, and center points to evaluate the effects of the factors and their interactions.

3.2.2 Factors Considered for Optimization

The factors considered for optimization were:

- pH of the wastewater
- Contact time between the nanoparticles and wastewater
- Adsorbent dosage of the nanoparticles

3.2.3 Experimental Results

The treatment process was conducted according to the designed experiments, and the results from the 20 runs were obtained as shown in Table 3.2. These results include the percentage adsorption of contaminants, which were used to develop the response surface model.

Table 3.2: Results of the 20 experimental runs

Run	A: Dosage (g/L)	Time (minute)	pH	Contaminant removal (%)
1	8.17572	30.2024	8.78381	67.1092
2	1	52.5	7	22.6767
3	5.5	90	7	79.1423
4	2.82428	74.7976	8.78381	59.7323
5	2.82428	30.2024	5.21619	92.5546
6	5.5	52.5	7	99.8929
7	8.17572	30.2024	5.21619	55.2869
8	5.5	52.5	7	99.8929
9	2.82428	30.2024	8.78381	69.5546
10	5.5	52.5	7	90.8929
11	8.17572	74.7976	8.78381	87.5546
12	5.5	52.5	10	86.2505
13	5.5	52.5	4	78.4111
14	8.17572	74.7976	5.21619	54.0023
15	10	52.5	7	17.0899
16	5.5	52.5	7	99.8929
17	2.82428	74.7976	5.21619	60.6617
18	5.5	15	7	86.8758
19	5.5	52.5	7	99.8929

20	5.5	52.5	7	99.8929

3.2.4 Visual Assessment of Treated Wastewater

The visual appearance of the industrial paint wastewater was assessed before and after treatment with CaO nanoparticles (CaO-NPs) synthesized from snail shells. Initially, the wastewater exhibited a turbid and colored appearance, characteristic of suspended and dissolved contaminants present in the untreated wastewater. However, after treatment with CaO-NPs, a significant visual improvement was observed. The treated wastewater appeared clear and colorless, indicating the effective removal of contaminants by the CaO-NPs. This visual transformation demonstrates the efficacy of CaO-NPs as an adsorbent for contaminants removal in industrial paint wastewater.

Fig. 3.12: Industrial paint wastewater before treatment

Fig. 3.13: Industrial paint wastewater after treatment

3.3 Statistical and Graphical Analysis of the Experimental Results

3.3.1 Analysis of Variance (ANOVA)

Analysis of variance (Table 3.3) was used to evaluate the significance of the quadratic model. The application of design expert software was to design the experiments, and randomize the runs. Randomization makes the process parameters (factors) in one run neither depend on the process parameter of the previous runs nor predict the conditions in the subsequent run. The different process parameters such as paint wastewater pH, adsorbent dosage, and contact time in the adsorption percentage of the contaminants were generated in the model and optimized by response surface methodology. The adequacy and significance of the quadratic model were determined by analysis of variance (ANOVA). The ANOVA Table 3.3 provides information on the significance of each factor and their interactions.

Table 3.3: ANOVA for Quadratic model

Response 1: % Contaminant Removal

Source	Sum of Squares	df	Mean Square	F-value	p-value	
Model	11244.88	9	1249.43	39.42	< 0.0001	significant
A-CaO dosage	57.19	1	57.19	1.80	0.2089	
B-Time	92.59	1	92.59	2.92	0.1182	
C-pH	87.81	1	87.81	2.77	0.1270	
AB	463.24	1	463.24	14.61	0.0034	
AC	600.38	1	600.38	18.94	0.0014	
BC	239.81	1	239.81	7.57	0.0205	
A^2	9669.18	1	9669.18	305.05	< 0.0001	
B^2	185.14	1	185.14	5.84	0.0363	
C^2	210.74	1	210.74	6.65	0.0275	
Residual	316.97	10	31.70			
Lack of Fit	249.47	5	49.89	3.70	0.0889	not significant
Pure Error	67.50	5	13.50			
Cor Total	11561.85	19				

The ANOVA results for the quadratic model of the treatment process are presented below:

Overall Model Fit:

The model is significant with an F-value of 39.42 and a p-value less than 0.0001, indicating that the model is a good fit for the data.

Individual Factor Effects:

A-CaO dosage, B-Time, and C-pH have p-values greater than 0.05, indicating that they are not statistically significant factors in the model.

AB, AC, BC, A^2, B^2, and C^2 have p-values less than 0.05, indicating that they are statistically significant factors in the model.

Residual Analysis:

The lack of fit p-value is 0.0889, which is greater than 0.05, indicating that the lack of fit is not significant relative to the pure error.

The pure error is 13.50, indicating the variability within each factor level combination.

Overall Model Summary:

The model explains a significant amount of the variability in the response (% Contaminant Removal) with a high R-squared value.

These results suggest that factors AB, AC, BC, A^2, B^2, and C^2 have a significant impact on the contaminant removal efficiency, while factors A-CaO dosage, B-Time, and C-pH have no significant effect on the response.

3.3.2 Fit Statistics

Fit statistics, such as the coefficient of determination (R^2), adjusted R^2, and lack of fit, were calculated to assess the adequacy of the quadratic model in representing the experimental data.

Table 3.4: Fit Statistics for the quadratic model

R^2	0.9726
Adjusted R^2	0.9479
Predicted R^2	0.8287
Adequate Precision	19.2676
Std. Dev.	5.63
Mean	75.36
C.V. %	7.47

R-squared (R^2): The R-squared value of the model is 0.9726, indicating that approximately 97.26% of the variability in the response variable (% Contaminant Removal) can be explained by the model.

Adjusted R-squared: The adjusted R-squared value of the model is 0.9479, which considers the number of predictors in the model. This value suggests that the model is a good fit for the data.

Predicted R-squared: The predicted R-squared value of the model is 0.8287, indicating that the model can effectively predict the response variable.

Adequate Precision: The adequate precision of the model is 19.2676, which measures the signal-to-noise ratio. A value greater than 4 is desirable, indicating that the model can be used to navigate the design space.

Standard Deviation: The standard deviation of the response variable is 5.63, indicating the average deviation of the observed values from the predicted values by the model.

Mean: The mean of the response variable is 75.36, providing a reference point for the response variable's distribution.

Coefficient of Variation (C.V. %): The coefficient of variation is 7.47%, indicating the relative variability of the response variable.

The Predicted R^2 of 0.8287 is in reasonable agreement with the Adjusted R^2 of 0.9479; i.e. the difference is less than 0.2. Adequate Precision measures the signal to noise ratio. A ratio greater than 4 is desirable. The ratio of 19.268 indicates an adequate signal. This model can be used to navigate the design space.

3.3.3 Response Surface Model

The response surface model in terms of coded factors describes the relationship between the factors (A-Adsorbent dosage, B-Time, C-pH) and the response variable (%Contaminant Removal). The final equation for the model is as follows:

Final Equation in Terms of Coded Factors

% Contaminant Removal =

+98.11

-2.05 A

-2.60 B

+2.54 C

+7.61 AB

+8.66 AC

+5.48 BC

-25.90 A^2

-3.58 B^2

-3.82 C^2

This equation can be used to predict the % contaminants removal efficiency at any combination of the coded factor levels within the experimental range. By default, the high levels of the factors are coded as +1 and the low levels are coded as -1. The coded equation is useful for identifying the relative impact of the factors by comparing the factor coefficients.

3.4 Interpretation of Results

The results of the optimization process were interpreted using 3D response surface plots. These plots visualize the effects of the factors and their interactions on the adsorption efficiency of the CaO nanoparticles. The 3D response surface plot illustrates the relationship between two factors

and the response variable (contaminant removal efficiency) while keeping the third factor constant at its optimal level.

3.4.1 Interaction effects of CaO-NPs dosage and Contact Time (AB)

The combined effects of CaO-NPs and contact time (AB) on the percent removal of the contaminants are indicated in Fig. 3.14. From the plot, the percent removal of contaminants showed an increasing trend as the contact time increases and also increased with increasing adsorbent dosage and then started declining after attaining the optimal condition.

3.4.2 Interaction effect of CaO-NPs and pH (AC)

The interaction effect of CaO-NPs and pH (AC) was illustrated in the 3D response surface plot shown in Fig.3.15. The efficiency of the contaminant removal increases steadily with increase in pH of the wastewater sample and also increased with increasing CaO-NPs dosage and then started declining after attaining the optimal condition.

3.4.3 Interaction effects of time and pH (BC)

The interaction effect of tine and pH (BC) was depicted in the 3D response surface plot shown in Fig. 3.16. The flat and red appearance of the 3D response surface graph for the interaction effects of time (B) and pH (C) suggests that there is minimal to no interaction between these two factors in influencing contaminants removal efficiency. This indicates that changes in pH within the range tested have little effect on contaminants removal efficiency when contact time is varied. The flatness of the graph suggests that increasing or decreasing pH at different contact times does not significantly impact contaminants removal efficiency.

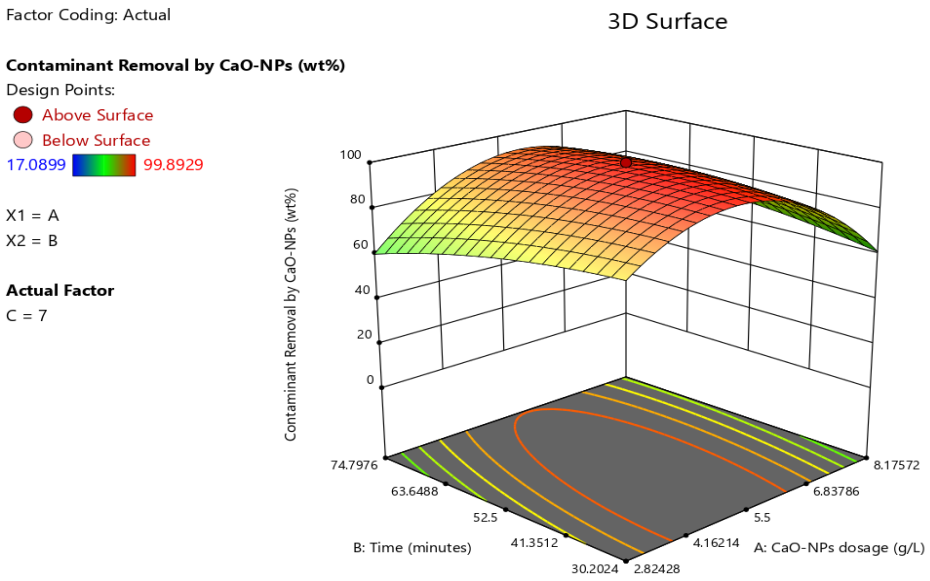

Fig. 3.14: 3D Response surface plot showing the interaction effects of CaO-NPs dosage and Contact Time (AB) on contaminants removal

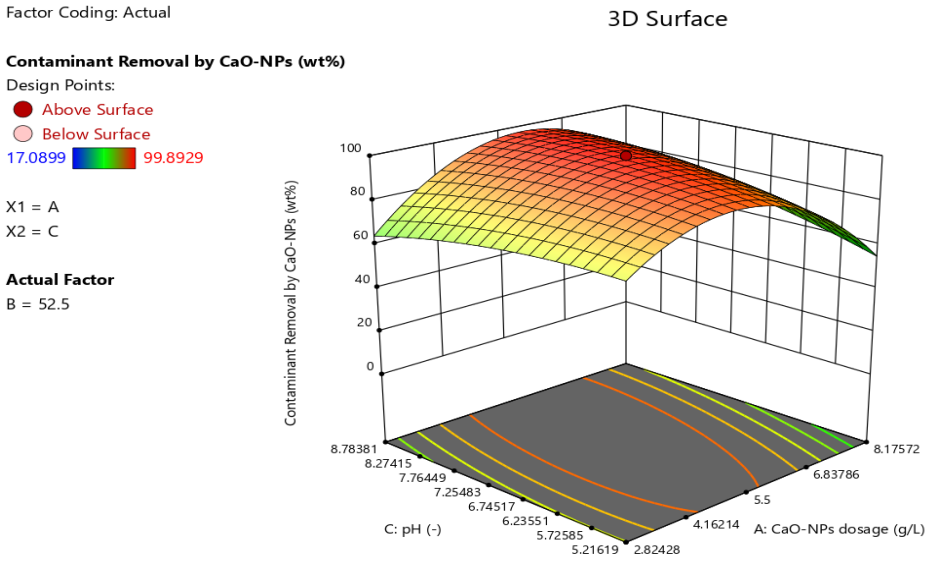

Fig. 3.15: 3D Response surface plot showing the interaction effects of CaO-NPs and pH (AC) on contaminants removal

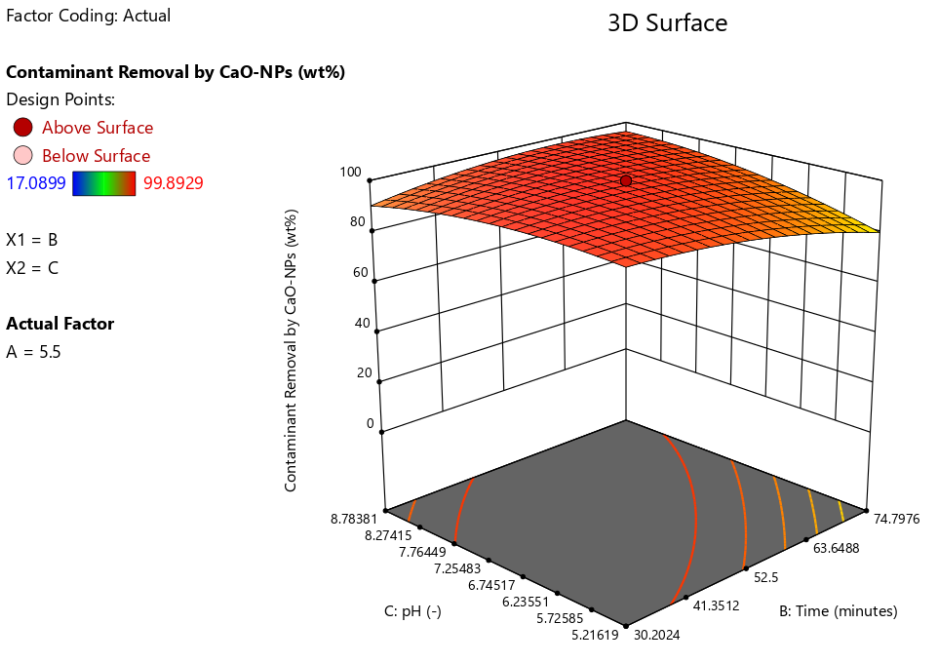

Fig. 3.16: 3D Response surface plot showing the interaction effects of time and pH (BC) on contaminants removal

3.4.4 Optimization Parameters of contaminants removal by CaO-NPs

The optimization of contaminants removal by CaO nanoparticles (CaO-NPs) was achieved using a desirability function that considered multiple factors. The optimal conditions for maximum contaminants removal efficiency were identified as follows; CaO-NPs Dosage (A): 5.5 g/L; Contact Time (B): 52.5 minutes; pH (C): 7

Under these optimal conditions, the contaminants removal efficiency by CaO-NPs was determined to be 98.1091%. These parameters represent the ideal combination for achieving maximum contaminants removal efficiency in the treatment of industrial paint wastewater using CaO nanoparticles.

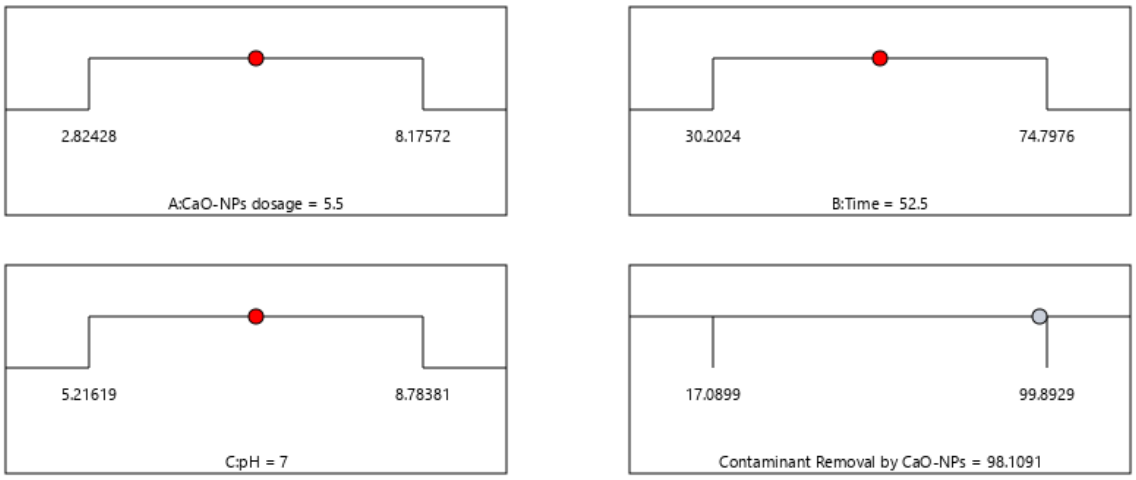

Fig. 3.17: Desirability Analysis for Contaminants Removal

3.4.5 Validation experiments

In order to verify the optimization results, an experiment was conducted under predicted conditions through the developed model. From Fig. 21, the model predicted 98.01% removal of contaminants at CaO-NPs dosage 5.5g/L, pH 7 and contact time 52.5min. Also, the experimental value obtained at these conditions of contaminants removal was 97.80% and was in close agreement with the result obtained from the model and hence validated the findings of the optimization. This experimental validation was the final step in the modeling process to investigate the accuracy of the established models. The maximum error (%) between the predicted and the experimental values was 0.21%, which is less than 3%, indicating that the quadratic models adopted could predict the experimental result well (*Okolo et al., 2020*). Hence, it can be concluded that the models accurately represent lead (II) ion removal over the experimental range studied.

3.5 Conclusion

The synthesis, optimization, and application of CaO nanoparticles (CaO-NPs) for the treatment of industrial paint wastewater have been successfully investigated. The sol-gel method was employed to synthesize CaO-NPs from snail shells, providing a sustainable and cost-effective approach to nanoparticle production. The characterization of the synthesized nanoparticles using X-ray Diffraction (XRD) analysis confirmed the crystalline nature of the nanoparticles, while Dynamic Light Scattering (DLS) provided valuable information about their size distribution and stability. Additionally, Fourier Transform Infrared (FTIR) spectroscopy revealed the presence of characteristic functional groups, further supporting the successful synthesis of CaO nanoparticles. The optimization of treatment conditions using response surface methodology (RSM) with central composite design (CCD) resulted in the identification of optimal conditions for contaminants removal. The desirability analysis revealed that a CaO-NPs dosage of 5.5 g/L, a contact time of 52.5 minutes, and a pH of 7 yielded a contaminants removal efficiency of 98.1091%. Validation experiments further confirmed the reliability and reproducibility of the optimized conditions, highlighting the robustness of the developed methodology. The results of the validation experiments support the practical implementation of CaO-NPs for industrial wastewater treatment, offering a sustainable and efficient solution for environmental remediation. One of the significant outcomes of this research is the remarkable visual improvement in the treated paint wastewater. The initially turbid and colored paint wastewater sample was transformed into a clear and colorless solution after treatment. This visual transformation not only demonstrates the efficacy of CaO-NPs as an adsorbent but also highlights the potential for their practical application in industrial wastewater treatment.

3.5.1 Contribution to Knowledge

- This study significantly contributes to the field of wastewater treatment by providing a novel and sustainable approach to the removal of contaminants from industrial paint wastewater.
- The successful synthesis of CaO nanoparticles (CaO-NPs) from snail shells using the sol-gel method showcases the potential of utilizing waste materials for nanoparticle production, thereby reducing environmental impact and promoting resource efficiency.
- The optimization of treatment conditions using response surface methodology (RSM) with central composite design (CCD) has demonstrated the effectiveness of CaO-NPs in achieving high removal efficiencies. The findings of this study highlight the importance of considering multiple factors, such as dosage, contact time, and pH, in wastewater treatment optimization, providing a valuable methodology for future research and applications in the field.

Overall, this study expands the current understanding of nanoparticle synthesis and application in wastewater treatment, emphasizing the potential for sustainable and cost-effective treatment solutions. By integrating principles of green chemistry and nanotechnology, this research contributes to the development of innovative and environmentally friendly approaches to water quality management.

3.6 Recommendations

- **Scale-Up and Practical Implementation:** Further research is needed to scale up the synthesis process of CaO-NPs and assess their practical implementation in industrial-scale wastewater treatment plants. This includes evaluating the cost-effectiveness, efficiency, and environmental impact of large-scale CaO-NPs production and application
- **Optimization in Different Wastewater Matrices:** The application of CaO-NPs should be explored in other wastewater matrices to assess their effectiveness and efficiency across different industrial sectors. This includes investigating the treatment of wastewater from other industries such as textiles, pharmaceuticals, and food processing.
- **Long-Term Stability and Reusability:** Studies on the long-term stability and reusability of CaO-NPs in wastewater treatment are essential to assess their practical feasibility and environmental sustainability. This includes evaluating the potential for regeneration and reuse of CaO-NPs to reduce waste generation and enhance cost-effectiveness.
- **Environmental Impact Assessment:** Comprehensive environmental impact assessments should be conducted to evaluate the potential environmental risks and benefits associated with the application of CaO-NPs in wastewater treatment. This includes assessing their impact on aquatic ecosystems, soil quality, and human health.

REFERENCES

Abid, N., Khan, A.M., Shujait, S., Chaudhary, K., Ikram, M., Imran, M. (2021). Synthesis of nanomaterials using various top-down and bottom-up approaches, influencing factors, advantages, and disadvantages: a review. Advances in Colloid and Interface Science, 48(2), 135-141.

Afroze, S., Sen, T. (2018). A review on heavy metal ions and dye adsorption from water by agricultural solid waste adsorbents. Water, Air, and Soil Pollution, 229(1), 225-229.

Amato, R.D., Falconieri, M., Gagliardi, S., Popovici, E., Serra, E., Terranova, G. (2013). Synthesis of ceramic nanoparticles by Laser pyrolysis: from research to applications. Journal of Analytical and Applied Pyrolysis, (104), 461-469.

Andrievski, R.A. (2014). Review of thermal stability of nanomaterials. Journal of Materials Science, 49(4), 1449-1460.

Aniyikaiye, T.E. (2019). Physico-chemical analysis of wastewater discharge from selected paint industries in Lagos, Nigeria. International Journal of Environmental Research and Public Health, (16), 2405.

Araujo, R., Castro, A. C. M., Fiuza, A. (2015). The use of nanoparticles in soil and water remediation processes. Materials Today: Proceedings, 2(1), 315-320.

Banerjee, A.N., Krishna, R., Das, B. (2008). Size controlled deposition of Cu and Si nano-clusters by an ultra-high vacuum sputtering gas aggregation technique. Applied Physics A, 90, 299-303.

Bardestani, R., Patience, G.S., Kaliaguine, S. (2019). Experimental methods in chemical engineering: specific surface area and pore size distribution measurements—BET, BJH, and DFT. Canadian Journal of Chemical Engineering, 97(11), 2781-2791

Bratovcic, A. (2019). Different Applications of Nanomaterials and Their Impact on the Environment. International Journal of Materials Science and Engineering, 5(1), 1-7.

Buzea, C., Pacheco, I.I., Robbie, K. (2007). Nanomaterials and nanoparticles: sources and toxicity. Biointerphases, 2(4), 7-71.

Byun, H.J., Lee, J.C., Yang, H. (2011). Solvothermal synthesis of InP Quantum dots and their enhanced luminescent efficiency by post-synthetic treatments. Journal of Colloid and Interface Science, 48(2), 35-41.

Chaturvedi, V. K., Kushwaha, A., Maurya, S., Tabassum, N., Chaurasia, H., Singh, M. P. (n.d.). Wastewater Treatment Through Nanotechnology: Role And Prospects. Restoration of Wetland Ecosystems, 1(1), 1-10.

Chen, Y., Wang, L., Zhao, Y., Li, Y. (2020). Treatment of paint wastewater by a coupled process of AOPs and coagulation: A review. Journal of Hazardous Materials, 401(2), 123413.

Cho, H-H., Wepasnick, K., Smith, B.A., Bangash, F.K., Fairbrother, D.H., Ball, W.P. (2010). Sorption of aqueous Zn[II] and Cd[II] by multiwall carbon nanotubes: the relative roles of oxygen-containing functional groups and graphenic carbon. Langmuir, 26(2), 967-981.

Corsi, I., Winther-Nielsen, M., Sethi, R., Punta, C., Della Torre, C., Libralato, G., Cinuzzi, F. (2018). Ecofriendly nanotechnologies and nanomaterials for environmental applications: key issue

and consensus recommendations for sustainable and ecosafe nanoremediation. Ecotoxicology and Environmental Safety, (154), 237-244.

Das, S., Srivasatava, V.C. (2016). Synthesis and characterization of ZnO-MgO nanocomposite by co-precipitation method. Smart Science, 4(2), 190-195.

De Silva, L.F. (2016). Treatment of paint manufacturing wastewater by coagulation/electrochemical methods: proposals for disposal and/or reuse of treated water. Water Research, (91), 288-297.

Deliyanni, E.A., Kyzas, G.Z., Triantafyllidis, K.S., Matis, K.A. (2015). Activated carbons for the removal of heavy metal ions: A Systematic review of recent literature focused on lead and Arsenic ions. Open Chemistry, 13(1), 699-708.

Ealia, S.A.M., Saravanakumar, M.P. (2017). A review on the classification, characterization, synthesis of nanoparticles and their application. IOP Conference Series: Materials Science and Engineering, 32(1), 1-19.

El-sayed, M.E.A. (2020). Nanoadsorbents for water and wastewater remediation. Science of the Total Environment, 739(1), 1-10.

Epp, J. (2016). X-ray diffraction (XRD) techniques for materials characterization. In Materials Characterization Using Nondestructive Evaluation (NDE) Methods, 81-124

Fadley, C.S. (2010). X-ray photoelectron spectroscopy: progress and perspectives. Journal of Electron Spectroscopy and Related Phenomena, (178), 2-32.

Feinle, A., Elsaesser, M.S., Husing, N. (2016). Sol-gel synthesis of monolithic materials with hierarchical porosity. Chemical Society Reviews, 45(12), 3377-3399.

Feng, J., Tao, Y., Shen, X., Jin, H., Zhou, T., Zhou, Y., Lee, Y.I. (2019). Highly sensitive and selective fluorescent sensor for tetrabromobisphenol-A in electronic waste samples using molecularly imprinted polymer coated quantum dots. Microchemical Journal, (144), 93-101.

Feynman, R.P. (1959). There's Plenty of Room at the Bottom: An Invitation to Enter a New Field of Physics. APS Annual Meeting, 1959(1), 1-20.

Gade, A., Ingle, A., Whiteley, C., Rai, M. (2010). Mycogenic metal nanoparticles: Progress and applications. Biotechnology Letters, 32(5), 593-600.

Gross, J., Sayle, S., Karow, A.R., Bakowsky, U., Garidel, P. (2016). Nanoparticle tracking analysis of particle size and concentration detection in suspensions of polymer and protein samples: influence of experimental and data evaluation parameters. European Journal of Pharmaceutics and Biopharmaceutics, (104), 30-41.

Haruta, M. (2004). Nanoparticulate gold catalysts for low-temperature CO oxidation. ChemInform, 35(44), 8226.

Henry, C.R. (2005). Morphology of supported nanoparticles. Progress in Surface Science, 80(3-4), 92-116.

Huang, M., Yan, H., Chen, C., Song, D., Heinz, T.F., Hone, J. (2009). Phonon softening and crystallographic orientation of strained graphene studied by Raman spectroscopy. Proceedings of the National Academy of Sciences, 106(18), 7304-7308.

Huang, Y., Wang, C., Hu, S., Liu, Y. (2020). Enhanced removal of phosphate from wastewater using calcium oxide nanoparticles: Mechanism and influencing factors. Journal of Hazardous Materials, (383), 121210.

Jiang, L., Fang, L., Li, D. (2021). Mechanism and application of calcium oxide nanoparticles for treatment of dye-containing wastewater. Journal of Water Process Engineering, (44), 102307.

Kasirajan, R., Bekele, A., Girma, E. (2022). Adsorption of lead (Pb-II) using CaO-NPs synthesized by sol-gel process from hen eggshell: Response surface methodology for modeling, optimization and kinetic studies. South African Journal of Chemical Engineering, 40(2), 209-229.

Kelly, K.L., Coronado, E., Zhao, L.L., Schatz, G.C. (2003). The optical properties of metal nanoparticles: the influence of size, shape, and dielectric environment. Journal of Physical Chemistry B, 107(3), 668-677.

Khan, I., Saeed, K., Khan, I. (2019). Nanoparticles: properties, applications, and toxicities. Arab Journal of Chemistry, 12(7), 908-931.

Khin, M.M., Nair, A.S., Babu, V.J., Murugan, R., Ramakrishna, S. (2012). A review on nanomaterials for environmental remediation. Energy & Environmental Science, 5(8), 8075-8109.

Kim, J., Kang, M. (2020). Nanomaterials for wastewater treatment. Journal of Industrial and Engineering Chemistry, 81(1), 1-13.

Kolahalam, L.A., Viswanath, I.V.K., Diwakar, B.S., Govindh, B., Reddy, V., Murthy, Y.L.N. (2019). Review on nanomaterials: synthesis and applications. Materials Today: Proceedings, 18(2), 2182-2190.

Konyukhov, Y. V. (2018). Heavy-Metal Extraction from Wastewater by Means of Iron Nanopowder. Steel in Translation, 48(2), 135-Means

Kumar, C.V., Pattammattel, A. (2017). Chapter 2 – Synthetic routes to graphene preparation from the perspectives of possible biological applications. In Introduction to Graphene (pp. 17-44). Elsevier.

Li, Q., Zhang, Y., Wang, X., Chen, X. (2017). Sustainable synthesis of CaO nanoparticles from snail shells for wastewater treatment. ACS Sustainable Chemistry & Engineering, 5(10), 8321-8328.

Li, Z., Wang, Y., Shen, J., Liu, W., Sun, X. (2014). The measurement system of nanoparticle size distribution from dynamic light scattering data. Optics and Lasers in Engineering, 56, 94-98.

Manor, J., Feldblum, E.S., Zanni, M.T., Arkin, I.T. (2012). Environment polarity in proteins mapped noninvasively by FTIR spectroscopy. Journal of Physical Chemistry Letters, 3(7), 939-944.

Mauter, M.S., Elimelech, M. (2008). Environmental applications of carbon-based nanomaterials. Environmental Science & Technology, 42(16), 5843-5859.

Mauter, M.S., Zucker, I., Perreault, F., Werber, J.R., Kim, J.H., Elimelech, M. (2018). The role of nanotechnology in tackling global water challenges. Nature Sustainability, 1, 166.

Méndez, E., González-Fuentes, M.A., Rebollar-Perez, G., Méndez-Albores, A., Torres, E. (2017). Emerging pollutant treatments in wastewater: cases of antibiotics and hormones. Journal of Environmental Science and Health, Part A, (52), 235-253.

Meshesha, B.T., Barrabes, N., Medina, F., Sueiras, J.E. (2009). Polyol mediated synthesis & characterization of Cu nanoparticles: effect of 1-hexadecylamine as stabilizing agent. Nanotechnology, 1(4).

Mohammadzadeh, V., Barani, M., Amiri, M.S., Yazdi, M.E., Hassanisaadi, M., Rahdar, A. (2022). Applications of plant-based nanoparticles in nanomedicine: a review. Sustainable Chemistry and Pharmacy, (25), 100606.

Mostafaie, A., Cardoso, D., Kamali, M., Loureiro, S. (2021). A Scientometric Study on Industrial Effluent and Sludge Toxicity. Toxics, 9(2), 176-186.

Mulvaney, P. (2015). Nanoscience vs nanotechnology—defining the field. ACS Nano, 5(2), 1-18.

Narayanan, K.B., Sakthivel, N. (2010). Biological synthesis of metal nanoparticles by microbes. Advances in Colloid and Interface Science, 156(1-2), 1-13..

Nicholas, J. (2018). Environmental impact of the paint manufacturing industry. Journal of Environmental Chemistry, 12(3), 45-56.

Nizamuddin, S., Siddiqui, M. T. H., Mubarak, N. M., Baloch, H. A., Abdullah, E. C., Mazari, S. A., Tanksale, A. (2018). Iron oxide nanomaterials for the removal of heavy metals and dyes from wastewater. In Nanoscale Materials in Water Purification . 1(4), 267-294 Elsevier Inc.

Pan, K., Zhong, Q. (2016). Organic nanoparticles in foods: fabrication, characterization, and utilization. Annual Review of Food Science and Technology, 7(1), 245-266.

Patel, S., Patel, P., Undre, S.B., Pandya, S.R., Singh, M., Bakshi, S. (2016). DNA binding and dispersion activities of titanium dioxide nanoparticles with UV/vis spectrophotometry, fluorescence spectroscopy and physicochemical analysis at physiological temperature. Journal of Molecular Liquids, (213), 304-311.

Pithawalla, Y. B., El-Shall, M. S., Deevi, S. C., Ström, V., Rao, K. V. (2001). Synthesis of magnetic intermetallic FeAl nanoparticles from a non-magnetic bulk alloy. Journal of Physical Chemistry B, 105(11), 2085-2090.

Qiu, L., Zhu, N., Feng, Y., Michaelides, E. E., Żyła, G., Jing, D. (2020). A review of recent advances in thermophysical properties at the nanoscale: from solid state to colloids. Physics Reports, 48(2), 1-81.

Rao, Y. N., Banerjee, D., Datta, A., Das, S. K., Guin, R., Saha, A. (2010). Gamma irradiation route to synthesis of highly re-dispersible natural polymer capped silver nanoparticles. Radiation Physics and Chemistry, (79), 1240-1246.

Rasalingam, S., Peng, R., & Koodali, R. T. (2014). Removal of hazardous pollutants from wastewaters: Applications of TiO2-SiO2 mixed oxide. Journal of Nanomaterials, 2014, 1–2.

Raval, R., Rangnekar, R. H., Raval, K. (2017). Optimization of chitosan nanoparticles synthesis and its applications in fatty acid absorption. Materials, Energy and Environment Engineering, 253-256..

Roduner, E. (2006). Size matters: why nanomaterials are different. Chemical Society Reviews, 35(7), 583-592.

Sharma, V. K., Filip, J., Zboril, R., Varma, R. S. (2015). Natural inorganic nanoparticles—formation, fate, and toxicity in the environment. Chemical Society Reviews, (44), 8410-8423.

Singh, T., Srivastava, N., Mishra, P.K., Bhatiya, A.K., Singh, N.L. (2016). Application of TiO2 Nanoparticle in Photocatalytic Degradation of Organic Pollutants. Materials Science Forum, 48(861), 1-12.

Thilakan, D., Patankar, J., Khadtare, S., Wagh, N.S., Lakkakula, J., El-Hady, K.M., Islam, S., Islam, M.R., Khan, M.S., Alafaleq, N.O., Tarique, M. (2022). Plant-Derived Iron Nanoparticles for Removal of Heavy Metals. International Journal of Chemical Engineering, 2022(1), 1-12.

Vladár, A. E., Hodoroaba, V.-D. (2020). Characterization of nanoparticles by scanning electron microscopy. In Characterization of Nanoparticles (pp. 7-27). Elsevier.

Wang, C., Liu, H., Zhang, G. (2020). Treatment of paint wastewater by membrane filtration: Performance and mechanism. Separation and Purification Technology, (215), 275-283.

Watcharaporn, K., Opaprakasit, M., Pimpan, V. (2014). Effects of UV radiation and pH of tannic acid solution in the synthesis of silver nanoparticles. Advanced Materials Research, (911), 110-114.

Wu, Q., Miao, W., Gao, H., Hui, D. (2020). Mechanical properties of nanomaterials: a review. Nanotechnology Reviews, 9(1), 259-273.

Yang, Y., Liu, X., Wang, X., Zhang, Y. (2020). Minimization of secondary waste by CaO nanoparticles in wastewater treatment. Journal of Environmental Management, 261(1), 110-117.

Zhang, Y., Wang, S., Ma, Y., Li, H., Wang, X. (2020). Adsorption of heavy metal ions from wastewater using surface-functionalized calcium oxide nanoparticles: Performance and mechanism. Chemical Engineering Journal, (400), 125949.

Zhang, Z., Zhang, Y., Lin, S., Lin, K., Li, J., Zhang, L., Liu, Y. (2019). Mechanism of calcium oxide nanoparticles in treating chromium-containing wastewater. Journal of Environmental Sciences, 79(2), 40-51.

Zhou, Y., Qu, Z. B., Zeng, Y., Zhou, T., & Shi, G. (2014). A novel composite of graphene quantum dots and molecularly imprinted polymer for fluorescent detection of paranitrophenol. Biosensors and Bioelectronics, (52), 317-323.